Geomorphological record of the glacial to periglacial transition from the Bølling–Allerød to the Holocene in the Central Pyrenees: the Lòcampo cirque in the regional context

Marcelo Fernandes, Marc Oliva, José María Fernández-Fernández, Gonçalo Vieira, David Palacios, Julia Garcia-Oteyza, Josep Ventura, Irene Schimmelpfennig, ASTER Team

BOREAS An international journal of Quaternary research

Geomorphological record of the glacial to periglacial transition from the Bølling–Allerød to the Holocene in the Central Pyrenees: the Lòcampo cirque in the regional context

MARCELO FERNANDES, MARC OLIVA, JOSÉ MARÍA FERNÁNDEZ-FERNÁNDEZ, GONÇALO VIEIRA, DAVID PALACIOS, JULIA GARCIA-OTEYZA, JOSEP VENTURA, IRENE SCHIMMELPFENNIG AND ASTER TEAM

BOREAS

Fernandes, M., Oliva, M., Fernández-Fernández, J. M., Vieira, G., Palacios, D., Garcia-Oteyza, J., Ventura, J., Schimmelpfennig, I.& ASTER Team. 2024 (January): Geomorphological record of the glacial to periglacial transition from the Bølling–Allerød to the Holocene in the Central Pyrenees: the Lòcampo cirque in the regional context. *Boreas*, Vol. 53, pp. 71–87. https://doi.org/10.1111/bor.12633. ISSN 0300-9483.

In the highest tributaries of the Upper Garonne Basin, Central Pyrenees, cirques up to 2600 m a.s.l. were already deglaciated by 15–14 ka. The long-term deglaciation during Termination-1 (T-1) was interrupted by glacial advances within the cirques during the Bølling–Allerød (B-A) interstadial and the Younger Dryas stadial. The cirques preserve a variety of glacial and periglacial landforms whose chronologies are poorly known. This study is focused on the Lòcampo cirque (42°38′06″N and 0°59′10″E), Upper Garonne Basin, where a detailed geomorphological map and ^{10}Be terrestrial cosmic ray exposure (CRE) dating allowed us to constrain the chrono-sequence between the glacial and periglacial domains. In the small Lòcampo cirque, a glacier formed a cirque moraine between 2200 and 2300 m a.s.l., which surrounds a relict rock glacier encompassing several transversal ridges. Additionally, longitudinal ridges typically observed in debris-covered glaciers are preserved between the moraine and the rock glacier. The eight-sample data set of CRE ages indicates the formation of the cirque moraine during the second half of the B-A, by 13.2±1.1 ka. Exposure ages from the rock glacier boulders show a range between 13.6±0.9 and 11.9±0.7 ka, which did not allow its formation to be chronologically constrained. Therefore, the environmental evolution following the moraine stabilization could follow the formation of a debris-covered glacier at the bottom of the Lòcampo cirque, with the subsequent formation of the rock glacier. After the rock glacier formation, its front rapidly ceased at 13.6±0.9 ka, while the upper ridges gradually stabilized until it became definitively relict at 11.9±0.7 ka or afterwards. These results show evidence of the complex glacial to periglacial transition that needs more robust chronological data sets to better understand the role of climate forcing and local topography during the deglaciation in mid-latitude mountain environments.

Marcelo Fernandes (marcelo.fernandes@live.com), Centre of Geographical Studies, Institute of Geography and Spatial Planning, Universidade de Lisboa, Rua Branca Edmée Marques, 1600-276, Lisboa, Portugal; Marc Oliva, Julia Garcia-Oteyza and Josep Ventura, Department of Geography, Universitat de Barcelona, Montalegre 6, 08001, Barcelona, Catalonia, Spain; José María Fernández-Fernández and David Palacios, Department of Geography, Universidad Complutense de Madrid, Calle del Profesor Aranguren, s/n. Facultad de Geografía e Historia, Ciudad Universitaria, 28040, Madrid, Spain; Gonçalo Vieira, Centre of Geographical Studies, Institute of Geography and Spatial Planning, Universidade de Lisboa, Rua Branca Edmée Marques, 1600-276, Lisboa, Portugal and Associated Laboratory Terra, Instituto Superior de Agronomia Tapada da Ajuda, 1349-017, Lisboa, Portugal; Irene Schimmelpfennig and ASTER Team, Aix-Marseille Université, CNRS, IRD, INRAE, Coll. France, UM 34 CEREGE, Aix-en-Provence, France; *received 2nd April 2023, accepted 21st July 2023.*

Millennial-scale warming events throughout the last deglaciation promoted glacier recession towards the upper catchments in mid-latitude mountain ranges, such as those of the Mediterranean basin (e.g. Hughes *et al.* 2006a, b; Palacios *et al.* 2022). The end of the Last Glacial Cycle (Termination-1; T-1) spans from the culmination of the Last Glacial Maximum (LGM) at 26–19 ka to the beginning of the Holocene at 11.7 ka (Clark *et al.* 2009; Vázquez-Riveiros *et al.* 2022). During this phase, the increase in summer insolation and unstable marine-based ice-sheet margins in the Northern Hemisphere triggered the release of a considerable number of icebergs (Denton *et al.* 2010). As a result of an important freshwater input delivered into the North Atlantic Ocean, the Atlantic Meridional Overturning Circulation weakened and favoured the occurrence of cold spells such as the Oldest Dryas or Heinrich Stadial-1 (HS-1 ~18.2–14.6 ka; Toucanne *et al.* 2015) and Younger Dryas (YD: 12.9–11.7 ka; Rasmussen *et al.* 2014). On the contrary, a possible intensification of the Atlantic Meridional Overturning Circulation forced an abrupt warm period between these stadials (14.6 and 12.9 ka), known as Bølling–Allerød (B-A; Rasmussen *et al.* 2014; Obase & Abe-Ouchi 2019; Capron *et al.* 2021).

These large climatic variations during T-1 promoted an accelerated glacial recession in the high mountains of the Mediterranean basin that was interrupted by glacial advances during short-lived millennial and centennial-scale cold-climate events. These oscillations have been spatially reconstructed and chronologically constrained in some locations based on geomorphological evidence (e.g. García-Ruiz *et al.* 2016; Palacios *et al.* 2017a; Allard *et al.* 2021). As glaciers retreated, ice-free terrain became gradually affected by non-glacial geomorphological

DOI 10.1111/bor.12633

dynamics through periglacial, slope and alluvial processes, which were particularly intense during the paraglacial phase (Ballantyne 2002; Oliva *et al*. 2019). This glacial landscape adjustment implied a new slope morphology since the glacial deposits and debris derived from rock wall debuttressing contributed to a new organization of deposits and processes (Ballantyne 2002; McColl 2012). In highland permafrost areas from mid-latitude mountains, the enhanced warming favoured widespread rock slope failures (Krautblatter *et al*. 2012; Oliva *et al*. 2019).

In mountain regions, a wide range of glacial, paraglacial and periglacial features resulted from the gradual recession of glaciers during the last stages of the deglaciation. Most of these are still preserved in the highest areas and provide valuable palaeoclimatic and palaeoenvironmental data to understand the timing and associated geomorphological dynamics of this phase (Hughes & Woodward 2009). Within the cirques, the shrinking glaciers abandoned moraines and left debris-rich glacial deposits on the slopes and bottoms of the cirques that led to the formation of rock glaciers, most of them of glacigenic origin (Knight 2019; Knight *et al*. 2019). However, an asymmetric intensity of the paraglacial activity, which is more evident in narrow cirques with steep rock walls, led to different debris coverage across cirque floors and slopes. In any case, the chronological framework of the transition from the glacial to periglacial domains is poorly known (Oliva *et al*. 2016).

In the Pyrenees, the spatial distribution of cirque floors shows a north–south and east–west elevation gradient. In the Eastern Pyrenees, cirque floors are located between 1300 and 2300 m a.s.l. (Delmas *et al*. 2015), whereas in the Central Pyrenees they are higher, 1600–2800 m a.s.l. on the northern slopes and 1800–3000 m a.s.l. on the southern ones (Lopes *et al*. 2018; García-Ruiz *et al*. 2020). The chronology of the cirques deglaciation was constrained by cosmic-ray exposure (CRE) dating, which suggested that most cirques with peaks under 2800–3000 m a.s.l. were completely deglaciated by the onset of the Holocene (Palacios *et al*. 2015a, b; Crest *et al*. 2017; Jomelli *et al*. 2020; Oliva *et al*. 2021; Reixach *et al*. 2021). In the highest cirques, glacial evidence preserved in the form of cirque moraines originated from several glacial advances or standstills during HS-1, B-A and YD (Palacios *et al*. 2015a, b; Jomelli *et al*. 2020; Fernandes *et al*. 2021b; Oliva *et al*. 2021; Reixach *et al*. 2021). Glacier recession following these glacial advances, probably under a continental climate, allowed the formation of rock glaciers in the deglaciated areas (Fernandes *et al*. 2018). Rock glaciers in the Central Pyrenees are mainly dispersed between 2100 and 2400 m a.s.l. on northern-facing valleys (e.g. Aran Valley) and between 2300 and 2600 m a.s.l. on the southern side of the range (e.g. Boí and Noguera Pallaresa valleys; Fernandes *et al*. 2018; Ventura 2020). Considering the present-day lower limit of the permafrost belt in the Pyrenees, the few active rock glaciers are located above 2600 m a.s.l. (northern flanks) and 2800 m a.s.l. (southern flanks; Serrano *et al*. 2001, 2006, 2011; González-García 2014). Most of the rock glaciers in the Pyrenees are relicts, although their chronological evolution remains poorly known.

The scarce studies on the European mountains that attempted to understand the period of stabilization or stagnation of rock glaciers by applying CRE methods showed a considerable variation of the ages (Moran *et al*. 2016; Andrés *et al*. 2018; Steinemann *et al*. 2020; Dlabáčková *et al*. 2023). The CRE dating of large rock glaciers composed of a succession of ridges and furrows demonstrated that the oldest ages were found in the lower sector and the youngest in the highest ridges, suggesting the time of rock glacier development (Frauenfelder *et al*. 2005; Rode & Kellerer-Pirklbauer 2012; Scapozza *et al*. 2014; Winkler & Lambiel 2018). On the other hand, present-day monitoring of inactive rock glaciers (or transitional; Delaloye & Echelard 2021) undergoing a degradation process in response to current warming reports frequent boulder adjustments (Gómez-Ortiz *et al*. 2019). This pattern occurred also in the past as revealed by CRE ages in relict rock glaciers yielding a wide range of ages that show that the transition towards the relict state can take several thousand years (Fernández-Fernández *et al*. 2020; Tanarro *et al*. 2021). In any case, the youngest age in a CRE data set from rock glaciers is indicative of the final stabilization of a specific ridge. In the Pyrenees, the first studies on rock glaciers from the eastern and central parts of the range indicate that they became stable during the transition from cold to warm periods, such as from the HS-1 to the B-A and from the YD to the Holocene (Andrés *et al*. 2018; Jomelli *et al*. 2020). During the B-A, the stabilization of frontal lobes between 2100 and 2400 m a.s.l. occurred at 14–13 ka in the Aránser and Duran valleys, Eastern Pyrenees (Palacios *et al*. 2015b; Andrés *et al*. 2018) and in the Gállego Valley, southern face of the Central Pyrenes (Palacios *et al*. 2015a, 2017b). Similarly, during the YD/Holocene transition, evidence of frontal lobe stabilization at elevations of 2200–2400 m a.s.l. by 12–11 ka was detected in the Aránser and Gállego valleys (Palacios *et al*. 2015b, 2017b). Throughout the Middle Holocene, stabilization of boulders in the frontal lobes of rock glaciers at ~2400 m a.s.l. occurred by 7 ka in the Ariège Valley and by 6–5 ka in the Gállego Valley (Palacios *et al*. 2017b; Jomelli *et al*. 2020). Finally, the stagnation (or stabilization) of boulders from the upper lobes above 2400 m a.s.l. occurred essentially during the Middle–Late Holocene; this is the case for rock glaciers that ceased activity by 8–7 ka in the Aránser Valley (Andrés *et al*. 2018) and by 1 ka in the Ariège Valley (Jomelli *et al*. 2020).

However, despite these works focusing on the Southern Pyrenees, little is known about the timing, process

and asynchronies of rock glacier formation on the northern slope of the Pyrenees. In order to contribute to the understanding of the chronology of relict rock glaciers, the objectives of this work are to: (i) reconstruct the chronology of the last glacial advance in the Lòcampo cirque, Central Pyrenees; (ii) constrain the chronology of the stabilization in a rock glacier located at 2200–2300 m a.s.l. within the cirque; and (iii) shed light on the factors, triggers and mechanisms that supported the shift from glacial-to-periglacial conditions during the last phase of the last deglaciation.

Study area

The Pyrenees are a mountain range dividing the Iberian Peninsula from the rest of the European continent. They stretch from the Mediterranean Sea to the Atlantic Ocean along ~400 km, with ~100 km width. The highest peaks are located in the central axis of the range, where many rise above 3000 m a.s.l. (e.g. Aneto Peak, 3404 m a.s.l.) and become gradually lower towards the western and eastern regions.

The Upper Garonne Basin is located in the Central Pyrenees and is administratively divided into two districts by the French and Spanish border. Whereas la Pique River drains the western French territory, the main Garonne River drains in the eastern Spanish part, in the Aran Valley. Both rivers flow northwards along typical U-shaped valleys carved out by glaciers during Quaternary glaciations. The highest interfluves show mainly NE-exposed cirques stretching from 2100 to 2400 m a.s.l. in the floors to over 3000 m a.s.l. in peaks above their headwalls (e.g. Molières Peak, 3009 m a.s.l.; Besiberri Nord Peak, 3007 m a.s.l.).

This study focuses on the eastern margin of the Ruda Valley – headwaters of the Garonne Basin – where the Lòcampo cirque is located, at 42°38′06″–42°38′27″N and 0°58′36″–0°59′10″E. The area extends over 800 m in length and 500 m in width between 2200 and 2644 m a.s.l. at the highest peak (Tuc de Lòcampo; Fig. 1). The bedrock is hornblende granodiorite and porphyritic granite from the Maladeta Batholith that intruded the Pyrenean Palaeozoic basement during the Carboniferous, at *c.* 300 Ma (Cochelin 2017). In contact with granitoids, the older Ordovician slates, marbles and hornfels are well marked, forming the concave slopes (>30°) of the Ruda Valley and the relatively flat area of the Bonaigua divide (~2000 m a.s.l.). This valley was shaped by glacial abrasion during at least the last two glaciations (129 ka and before 24–21 ka) when large glaciers reached the Pyrenean foreland (Fernandes *et al.* 2021a). During and following the LGM, the glacier retreated 95% of its length, reaching the cirque level by 15–14 ka, as shown by CRE dating in the Bacivèr cirque, next to Lòcampo cirque (Fernandes *et al.* 2021b; Oliva *et al.* 2021). At the Bonaigua meteorological station (2266 m a.s.l.; Servei Meteorològic de Catalunya), the mean annual air temperature was 3 °C and the annual precipitation reached ~1200 mm between 2000 and 2020. On the cirque bottom, snow lasts from October to June, recording frequently >200 cm of depth in late winter and early spring (Bonsoms *et al.* 2021). The Lòcampo cirque contains a large moraine system and a well-developed relict rock glacier that constitutes a representative study case to explore its origin and the chronological sequence of the transition between the glacial to periglacial domains in the Central Pyrenees (Fernandes *et al.* 2022; Fig. 1).

Methodology

The reconstruction of the glacial and postglacial dynamics at the Lòcampo cirque was based on complementary geomorphological and geochronological approaches. Fieldwork was conducted during the summer of 2020, when the terrain was snow free and allowed the best identification of the glacial and periglacial features and the collection of rock samples for CRE.

Geomorphology and sampling strategy

A detailed geomorphological map at 1:5000 scale was adapted from Fernandes *et al.* (2022) and prepared using ArcMap (Environmental Systems Research Institute). Mapping was based on the interpretation of 1-m resolution orthophotomaps and 1-m resolution LiDAR-derived digital elevation models from the Institut Cartogràfic i Geològic de Catalunya, supported by field work.

Glacial and periglacial features were targeted for dating based on the geomorphological map, with eight granodiorite rock samples collected with a hammer and chisel (Table 1). The criterion for the boulder sampling was limiting the risk of postglacial reworking (i.e. overturning) or burial. Hence, we sampled boulders well anchored in the moraine, far from the talus and on top of the ridges of the rock glacier, with the longest axis ranging between 2 and 9 m (Fig. 2). Rock splits 3–5 cm thick were extracted from flat and gentle surfaces at the top of the selected boulders. Five samples were collected from the cirque moraine (ARAN-47, ARAN-48, ARAN-49, ARAN-53 and ARAN-54) and one from the top of each of the three highest ridges of a rock glacier (ARAN-50, ARAN-51 and ARAN-52).

Sample processing and exposure age calculation

The quartz richness of the granodiorites from the Lòcampo cirque allowed the extraction of the *in situ*-produced cosmogenic nuclide ^{10}Be. Samples were crushed and sieved to the 125–500 μm fraction at the laboratory of Physical Geography of the Universidad Complutense de Madrid (Spain). Further physical and chemical sample processing was conducted at the

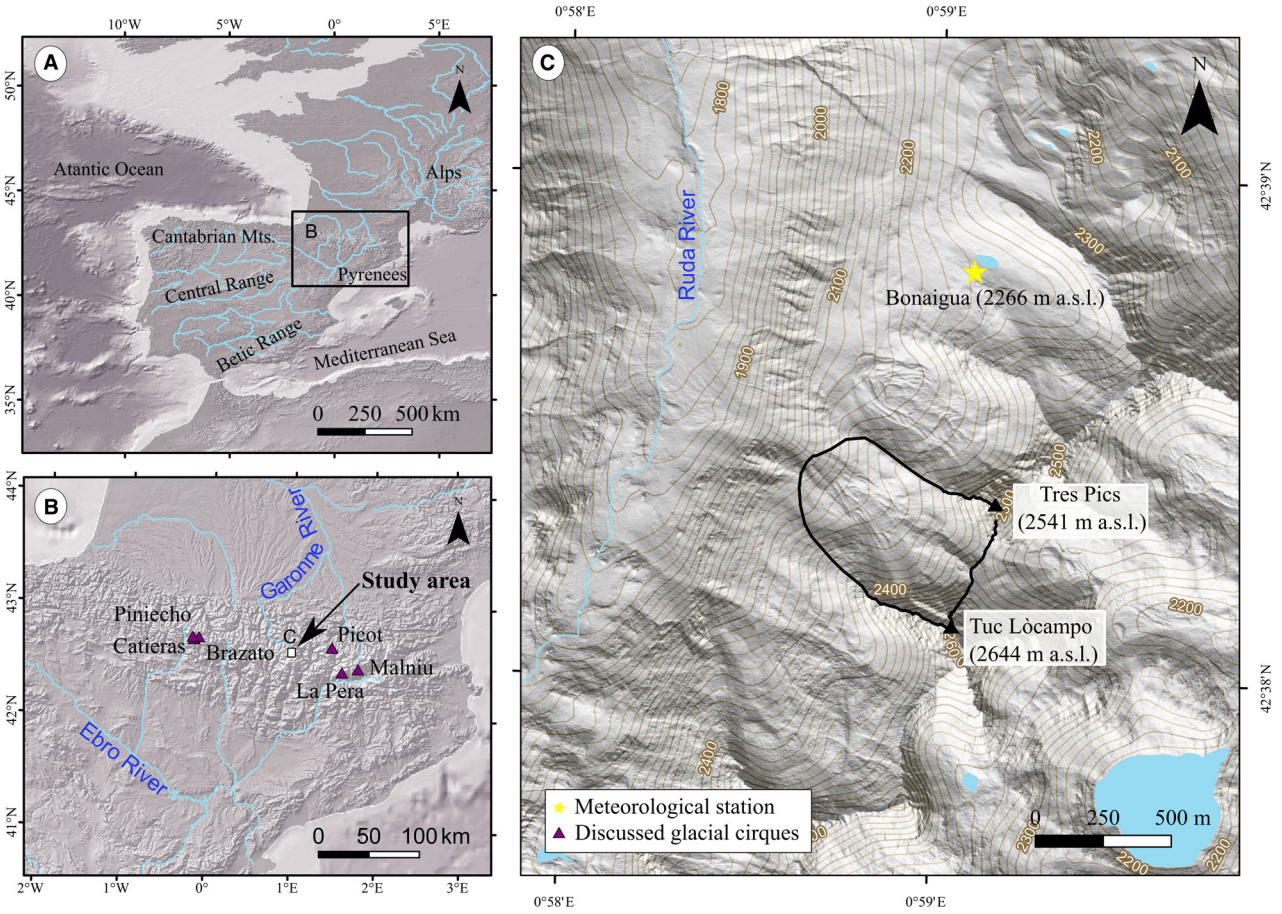

Fig. 1. Geographical setting of the Lòcampo cirque highlighted by the back line (C) within the Pyrenees (B) and within western Europe (A).

Table 1. Geographical location, topographical shielding factor and sample thickness of samples from boulders.

Sample name	Latitude (DD)	Longitude (DD)	Elevation (m a.s.l.)[1]	Topographic shielding factor	Thickness (cm)
Glacial cirque moraine					
ARAN-47	42.6399	0.9802	2236	0.9614	3.9
ARAN-48	42.6398	0.9802	2236	0.9708	2.3
ARAN-49	42.6397	0.9805	2240	0.9628	3.0
ARAN-53	42.6385	0.9836	2334	0.9238	4.5
ARAN-54	42.6385	0.9836	2332	0.9269	4.0
Rock glacier					
ARAN-50	42.6396	0.9797	2224	0.9714	3.8
ARAN-51	42.6393	0.9803	2236	0.9530	3.1
ARAN-52	42.6391	0.9818	2266	0.9501	4.0

[1]Elevations are derived from the 5-m digital elevation model of the Spanish Instituto Geográfico Nacional and are subjected to a vertical accuracy of ±5 m.

Laboratoire National des Nucléides Cosmogéniques of the Centre Européen de Recherche et d'Enseignement des Geosciences de l'Environnement (CEREGE; Aix-en-Provence, France). The final physical procedures focused on the removal of magnetic minerals by using a Frantz LB-1 magnetic separator.

In order to discard the remaining non-quartz minerals (e.g. feldspar), the non-magnetic fraction underwent several consecutive leachings of concentrated mixture of hydrochloric (1/3 HCl) and hexafluorosilicic (2/3 H_2SiF_6) acids and after that, atmospheric ^{10}Be was removed by successive partial dissolutions with concentrated hydrofluoric acid (HF). Subsequently, about 20 g of each sample was spiked with 150 µL on an in-house-manufactured ^{9}Be carrier solution (3025±9 µg ^{9}Be; Merchel *et al.* 2008). Finally, samples were totally

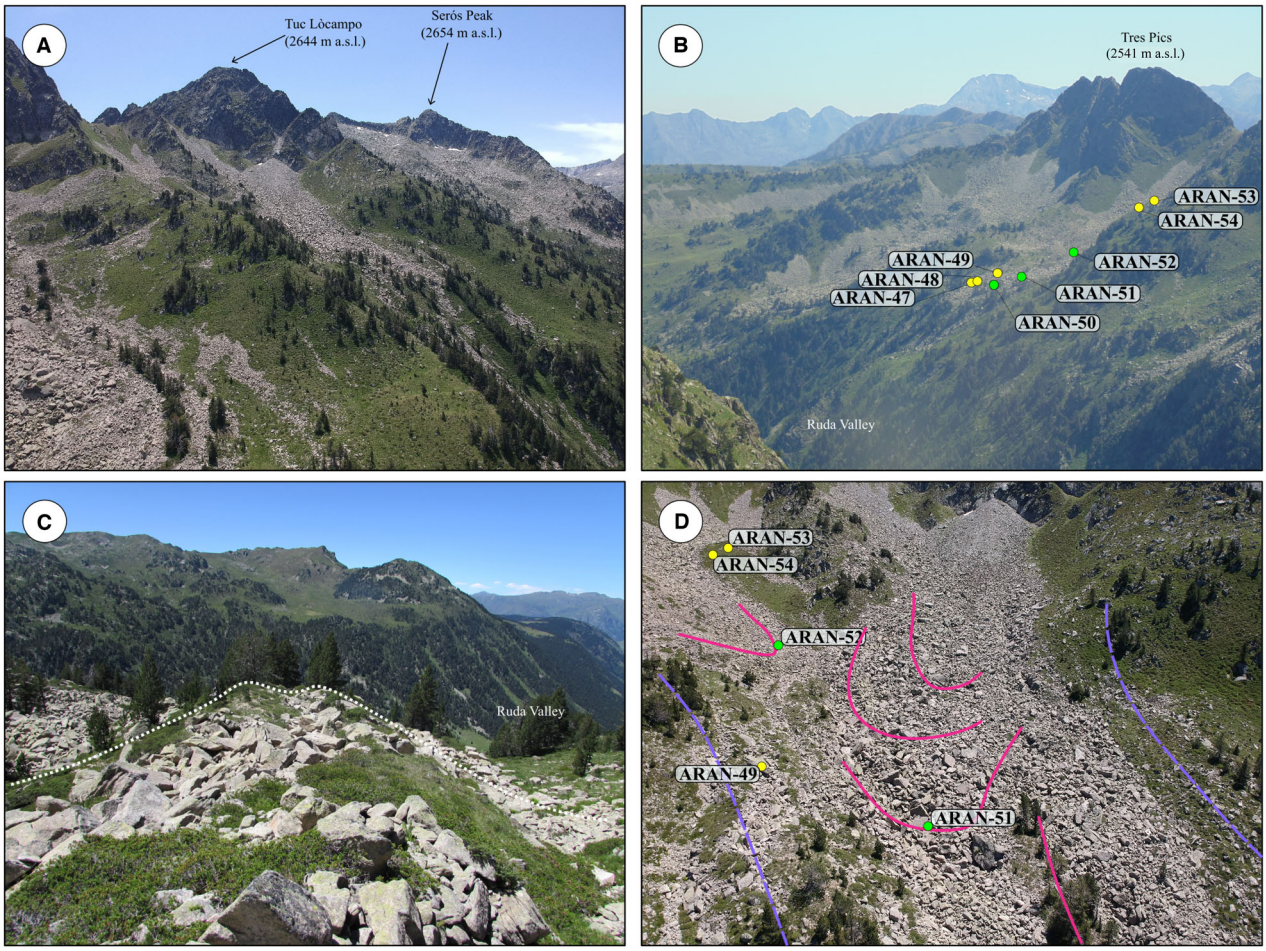

Fig. 2. Photographs of the Lòcampo cirque looking south (A) and north (B), as well as from the right ridge of the cirque moraine (C) and the rock glacier (D). In (D), the moraine crests are indicated by purple lines and the rock glacier ridges are marked with pink lines. Collected samples from moraine (yellow dots) and rock glacier (green dots) boulders are plotted in B and C.

dissolved in HF and Be was isolated using ion exchange columns and recovered as BeO (Merchel & Herpers 1999; Dunai 2010).

The BeO targets were mixed with niobium powder and loaded on copper cathodes for $^{10}Be/^{9}Be$ ratio measurements (Table 2) at the national accelerator mass spectrometer (AMS) facility ASTER at the CEREGE. The AMS measurements were calibrated against the in-house standard STD-11 with an assigned $^{10}Be/^{9}Be$ ratio of $1.191\pm0.013 \times 10^{-11}$ (Braucher *et al.* 2015).

The partial shielding of the surrounding reliefs was geometrically corrected by implementing a topographic shielding factor (Dunne *et al.* 1999), obtained from the ArcGIS toolbox developed by Li (2018). It requires the location of the sampling sites (point shapefile), the strike/dip angles of the sampled surfaces and a digital elevation model (a 5-m cell size was used for an efficient geoprocessing and calculation).

Exposure ages were calculated in the CREp online calculator (univ-lorraine.fr; Martin *et al.* 2017) with the Lifton–Sato–Dunai elevation/latitude scaling scheme (Lifton *et al.* 2014), ERA40 atmospheric model (Uppala *et al.* 2005), the geomagnetic database based on the Lifton–Sato–Dunai framework (Lifton *et al.* 2014) and the world wide mean production rate of 3.98 ± 0.22 atoms to $^{10}Be\ g^{-1}\ a^{-1}$ at sea level high latitude (Martin *et al.* 2017) to enable full comparison with the updated glacial chronology in the Iberian mountains (Oliva *et al.* 2022). The calculated exposure ages are shown in Table 2 together with the respective 1σ full and analytical uncertainties. The full error is presented with the ages unless otherwise stated.

Erosion correction was implemented through a conservative rate of 1 mm ka^{-1}, representative of the biotite-rich crystalline rock type (André 2002). On the other hand, snow shielding correction was based on equation 3.76 of Gosse & Phillips (2001), which is also included in Table 3. This equation considered 100 cm snow depth lasting for 7–8 months according to current data from the Bonaigua meteorological station and assumed a snow density of 0.2 g cm^{-3} (Styllas *et al.* 2018). Both corrections (snow and erosion) resulted

Table 2. AMS analytical data and exposure ages. $^{10}Be/^{9}Be$ ratios were inferred from measurements at the ASTER AMS facility. Individual ages are shown with their full uncertainties (including analytical AMS uncertainty and production rate uncertainty) and analytical uncertainty only within brackets. Arithmetic mean ages are given with their full uncertainties and standard deviations within brackets.

^{10}Be samples analytical AMS data								
Sample name	Quartz weight (g)	Mass of carrier (^{9}Be mg)	ASTER AMS cathode number	$^{10}Be/^{9}Be$ (10^{-14})	Blank correction (%)	^{10}Be (10^{4} atoms g^{-1})	Age (ka)	Mean age (ka)
Glacial cirque moraine								
ARAN-47	20.10	0.44	IGNM	18.09±0.57	1.07	26.25±0.83	12.6±0.8 (0.4)	13.7±1.5 (0.5)
ARAN-48	19.43	0.44	IGNN	18.21±0.64	1.06	27.33±0.97	12.9±0.8 (0.5)	
ARAN-49	20.38	0.44	IGNO	20.70±0.86	9.36	29.60±1.24	14.1±0.9 (0.6)	
ARAN-53	*20.63*	*0.44*	*IGNS*	*12.90±4.97*	*1.52*	*18.01±7.05*	*8.4±3.2 (3.2)*[1]	
ARAN-54	*20.01*	*0.44*	*IGNT*	*22.62±0.74*	*8.61*	*32.77±1.08*	*15.2±0.9 (0.4)*	
Rock glacier								
ARAN-50	21.01	0.44	IGNP	20.29±0.81	9.51	28.28±1.14	13.6±0.9 (0.5)	12.7±1.4 (0.4)
ARAN-51	21.03	0.44	IGNQ	17.71±0.59	1.09	24.55±0.83	11.9±0.7 (0.4)	
ARAN-52	20.50	0.44	IGNR	18.83±0.59	1.04	26.50±0.83	12.7±0.8 (0.4)	

Chemistry blank details				
Blank name	Mass of carrier (^{9}Be mg)	ASTER AMS cathode number	$^{10}Be/^{9}Be$ (10^{-14})	^{10}Be (10^{4} atoms)
ARAN BK	0.44	IGNV	0.20±0.03	5.65±0.84

[1]The exposure ages in italics were identified as outliers based on low measurement currents and high analytical uncertainty. These exposure ages were therefore not included in the interpretation.

in ~9% older ages with ~1% from erosion and ~8% from snow cover. However, as most of the published ages from other areas do not consider any correction, we used non-corrected ages. The chi-squared test was applied according to Ward & Wilson (1978) in the moraine units and the sample ARAN-54 (15.2±3.2 ka) was detected as an outlier. The high internal errors of the sample ARAN-53 (8.4±3.2 ka) owing to the low current during the AMS measurements implied rejection of this age.

Results

The geomorphological mapping revealed a significant variety of glacial and periglacial landforms in the Lòcampo cirque. Exposure ages provided the chronological framework of the moraine and rock glacier stabilization during the final phases of the last deglaciation (Fig. 3).

Geomorphological evidence

The Lòcampo glacial cirque is oriented towards NW and is relatively small (38 ha) compared with those in the rest of the Aran Valley (62 ha on average; Lopes *et al.* 2018). It is located on the western face of the arête dividing the Ruda and Gerber valleys. The steep headwall of the cirque is composed of 100–300 m rock walls (from ~2600 on the ridge to 2300 m a.s.l. at the foot) and includes two glacial overdeepenings separated by a rock ridge. On the sides of the Lòcampo cirque, interfluves at 2360–2200 m a.s.l. separating the adjacent cirques show glacially abraded surfaces with scattered erratic boulders. These interfluves become steeper towards the cirque floor where the rock walls are covered by talus debris and block streams. On the bottom of the cirque, an overdeepened depression (~300-m long, ~200-m wide) extends between 2300 and 2200 m a.s.l. where a moraine

Table 3. Exposure ages according to different erosion and snow cover correction scenarios. The ages in italic were considered outliers.

Sample name	Exposure ages (arithmetic mean, in ka)			
	No correction	Erosion correction	Snow correction	Erosion + snow correction
Glacial cirque moraine	13.2±11 (0.5)	13.3±1.2	14.2±1.2	14.4±1.2
ARAN-47	12.6±0.8 (0.4)	12.8±0.8 (0.4)	13.6±0.8 (0.4)	13.8±0.8 (0.4)
ARAN-48	12.9±0.8 (0.5)	13±0.8 (0.5)	13.9±0.9 (0.5)	14.1±0.9 (0.5)
ARAN-49	14.1±0.9 (0.6)	14.2±0.9 (0.6)	15.1±1 (0.6)	15.3±1 (0.6)
ARAN-53	*8.4±3.2 (3.2)*	*8.5±3.3 (3.2)*	*9.1±3.5 (3.5)*	*9.2±3.5 (3.5)*
ARAN-54	*15.2±0.9 (0.4)*	*15.4±0.9 (0.5)*	*16.4±1 (0.5)*	*16.6±1 (0.5)*
Rock glacier	12.7±1.4 (0.4)	12.9±1.2	13.7±1.2	13.9±1.3
ARAN-50	13.6±0.9 (0.5)	13.8±0.9 (0.5)	14.6±0.9 (0.6)	14.8±0.9 (0.6)
ARAN-51	11.9±0.7 (0.4)	12±0.8 (0.4)	12.8±0.8 (0.4)	12.9±0.8 (0.4)
ARAN-52	12.7±0.8 (0.4)	12.8±0.8 (0.4)	13.6±0.8 (0.4)	13.8±0.8 (0.4)

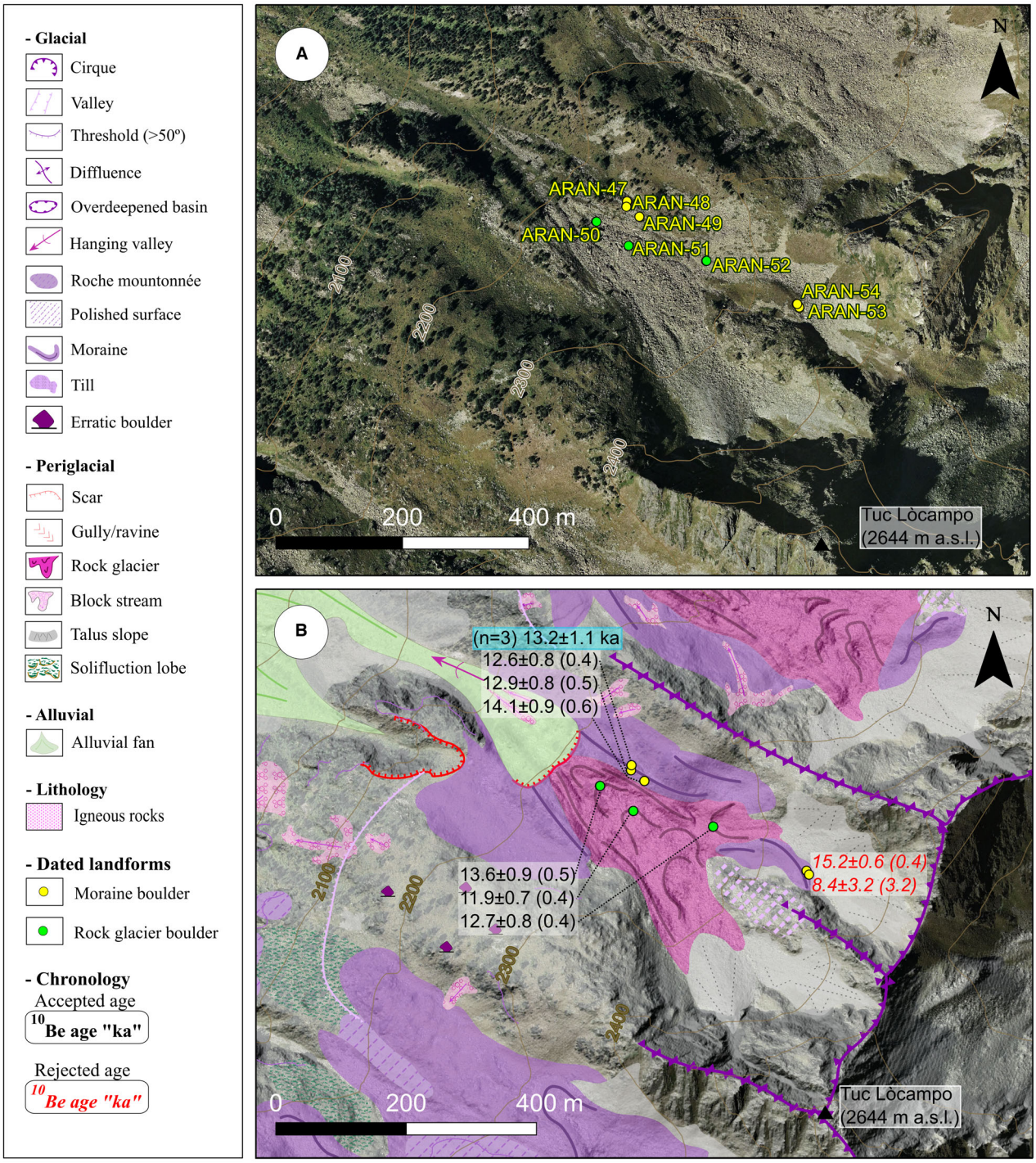

Fig. 3. Above, an orthophotomap from the Lòcampo cirque with the distribution of the samples and below, the geomorphological map with the distribution of the cosmic ray exposure (CRE) ages.

system is preserved. The Lòcampo cirque connects with the main Ruda Valley through a steep slope (>30°) of 400 m.

Two latero-frontal moraines close the lower margins of the cirque between 2290 and 2220 m a.s.l. The moraines are composed of metre-sized subangular to subrounded boulders embedded in a sandy matrix forming elongated 5-m-high ridges on the northern and southern margins of the cirque. These moraines are interpreted as remnants of an ancient frontal cirque moraine whose distal part is currently eroded. On these moraines, a sequence of two 2-m-high ridges oblique to the main one and composed of

large subrounded boulders with no matrix are interpreted as push moraines. On the forefront of the frontal moraine, the till is affected by a scar that cuts the moraine, evidencing that this section of the moraine was eroded by gravitational processes. Finally, on the north side of the rock ridge dividing the two glacial hollows there is another moraine ridge at 2340–2280 m a.s.l. which is composed of anchored boulders. Since this moraine stretches westwards, towards the centre of the cirque, it is probably a remnant of the highest cirque moraine reworked by the rock glacier dynamics (Fig. 3).

The sedimentological and morphological features of the cirque moraine show a very distinct change towards the centre of the Lòcampo cirque. In fact, the aforementioned moraine surrounds a 5-ha deposit containing 1–9 m long angular to subangular boulders lacking fine-grained sediments. This NW-oriented deposit (410 m long and 150 m wide) is considered a rock glacier and extends from 2330 to 2210 m a.s.l. Morphologically, it includes several >5-m-high ridges, perpendicular to the slope and divided by furrows that tend to be higher in the lower altitudes. In the upper sector of the rock glacier, two ridges ~5–12 m high are located at ~2280–2265 m a.s.l. and are separated by the glacial hollows of the cirque. The following well-defined ridge (~4–5 m high) is located at 2240–2235 m a.s.l. and lies in the central part of the rock glacier. Further down, at 2230–2220 m a.s.l., another ridge (~5–6 m high) narrows towards the front of the rock glacier. Finally, at 2215–2210 m a.s.l. the last ridge (~7–8 m high) is almost connected to the cirque moraine (Fig. 3). Finally, the forest on the rock glacier shows evidence that this feature is relict and it is located below the altitude of the currently active rock glaciers (~2650 m a.s.l.; e.g. Serrano *et al.* 2011) and continuous permafrost in the Pyrenees (~2800–3000 m a.s.l.; Serrano *et al.* 2019).

Between the margins of the cirque moraine and the rock glacier, there are longitudinal ridges that stretch parallel to both the northern and southern moraine ridges. These elongated ridges encompass angular to surrounded boulders embedded on a fine-grained matrix. Besides, the area between these ridges and the rock glacier is covered with debris, with no visible depression in between. Therefore, these moraine features might suggest a deposition during a phase of transition between the debris-free and the rock glacier, probably from a debris-covered glacier (Fernández-Fernández *et al.* 2017).

Geochronological data

The eight samples from the Lòcampo cirque yielded ages covering a 3-ka period representative of the final phases of the deglaciation in the Aran Valley, between 14.1±0.9 and 11.9±0.7 ka (Table 2, Fig. 4).

At the northern margin of the glacial cirque, the three samples from the cirque moraine (ARAN-47, ARAN-48 and ARAN-49) reported chronostratigraphically and statistically consistent ages: 12.6±0.8, 12.9±0.8 and 14.1±0.9 ka, which yield a mean age of 13.2±1.1 ka.

The three samples obtained from stable boulders of the highest ridges of the rock glacier (ARAN-50, ARAN-51 and ARAN-52) showed a geomorphologically consistent sequence of ages 13.6±0.9, 11.9±0.7 and 12.7±0.8 ka, considering the period of stabilization of the rock glacier (Amschwand *et al.* 2021; Lehmann *et al.* 2022).

Discussion

The ^{10}Be CRE age data set supported by the detailed geomorphological mapping allowed the development of a model of the glacial to periglacial transition in the Lòcampo cirque. The sampled boulders yielded ages spanning the second half of T-1.

Geomorphological interpretation and hypothesis construction

This study underpins the nonlinear long-term deglaciation in the Upper Garonne Basin during the T-1 that was proposed in earlier studies (Fernandes *et al.* 2017, 2021b, 2022; Oliva *et al.* 2021). The cirque moraine preserved in the Lòcampo cirque was probably formed by a debris-free glacier as it is significantly higher (~12–15 m) than the rock glacier ridges. Debris-free glaciers commonly form more prominent moraine features as they are usually thicker than the debris-covered ones (Haeberli 1985). The CRE ages from the cirque moraine in the Lòcampo cirque showed a mean of 13.2±1.1 ka. In data sets with relatively high scattered ages, the average provides a reasonable estimate for the true age of the moraine formation (Applegate *et al.* 2012). This age suggests the timing of moraine abandonment right after the glacier advance during the second half of the B-A.

Following the moraine abandonment, the debris-free glacier of the Lòcampo cirque probably evolved into a debris-covered one, the presence of longitudinal crests in contact with the internal margins of the moraine revealed (Clark *et al.* 1994). In addition, the overlap of CRE ages between the cirque moraine (13.2±1.1 ka) and the rock glacier (frontal ridge: 13.6±0.9 ka) might underline that those boulders were already emplaced on top of the glacier surface during the moraine stabilization. This would support the idea that the ice mass hosted in the Lòcampo cirque was debris covered before the rock glacier was formed. Since then, the intense debris supplied by the surrounding slopes during the paraglacial phase as well as the abundant material left by the debris-covered glacier have favoured the development of the rock glacier (Fig. 5). However, we cannot exclude that the rock glacier could have formed directly after the stabilization of the moraine. Such evolution could have occurred during the late B-A/early YD, as suggested by the similar ages from the cirque moraine and the oldest

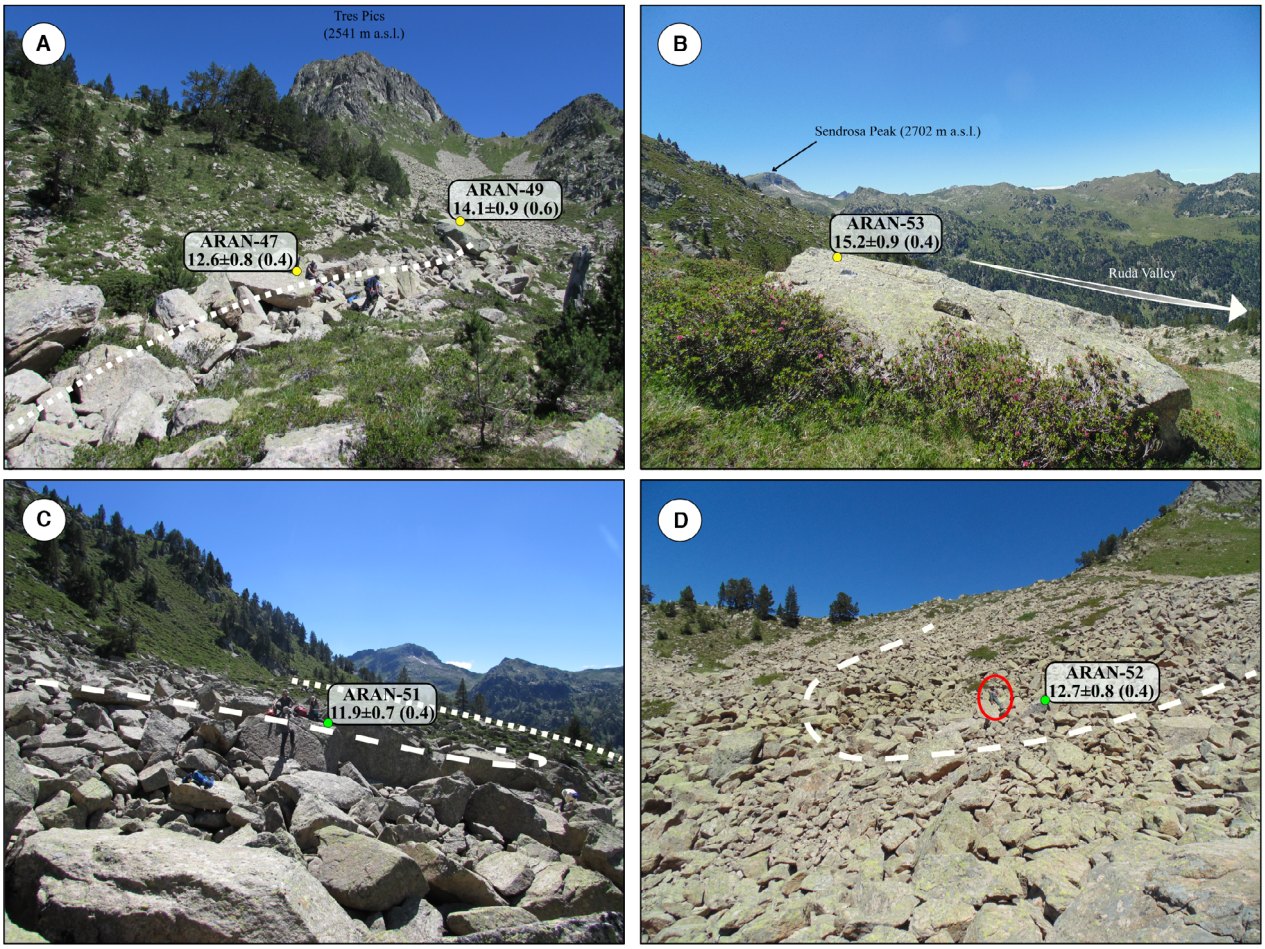

Fig. 4. Examples of landforms with the respective CRE ages. A. Northern ridge of the cirque moraine. B. Upper unit of the moraine system. C. Internal lobe of the rock glacier with the left ridge of the cirque moraine. D. Upper lobe of the rock glacier with the graphic scale of men size (black circle).

age of the rock glacier (see e.g. Fernández-Fernández *et al.* 2020; Tanarro *et al.* 2021). In any case, these scenarios need to be validated with further CRE dating in future studies.

The rock glacier located within the limits of the cirque moraine indicates that periglacial conditions compatible with permafrost occurrence replaced the glacial environment in the Lòcampo cirque. The exact timing of the rock glacier formation cannot be inferred owing to the overlapping of the exposure ages of the moraine (13.2±1.1 ka) and the rock glacier (frontal ridge, 13.6±0.9 ka). Moreover, the limited number of samples and the associated uncertainties hinder an exact chronological determination of the rock glacier stabilization. However, the age data set suggests a transitional period from the cessation of the rock glacier movement to its ultimate relict state. Therefore, it can be concluded that the rock glacier at the Lòcampo cirque ceased activity right after its development, during the late B-A/early YD, by 13.6±0.9 ka as the oldest CRE age of the data set (13.6±0.9 to 11.9±0.7 ka), which coincides with that of the frontal rock glacier ridge. This means that the rock glacier stabilization probably started right after its rock glacier formation and became finally relict by the onset of the Holocene or afterwards, at 11.9±0.7 ka. Finally, considering the full age range given by the uncertainties, this transitional state of the rock glacier spans between a few thousand years (2–3 ka) to as little as 0.1 ka. This period indicates the subsequent phase of boulder readjustments or displacements triggered by the degradation of buried ice and subsequent collapse that could potentially persist longer in the centre and thicker part of the rock glacier.

Finally, we cannot exclude the possibility that some boulders may have provided older ages owing to the retaining of an unknown amount of nuclide inheritance or even a more complex history considering the time of transport on the glacier surface after detachment from the rock walls (Anderson *et al.* 2018; Scherler & Egholm 2020).

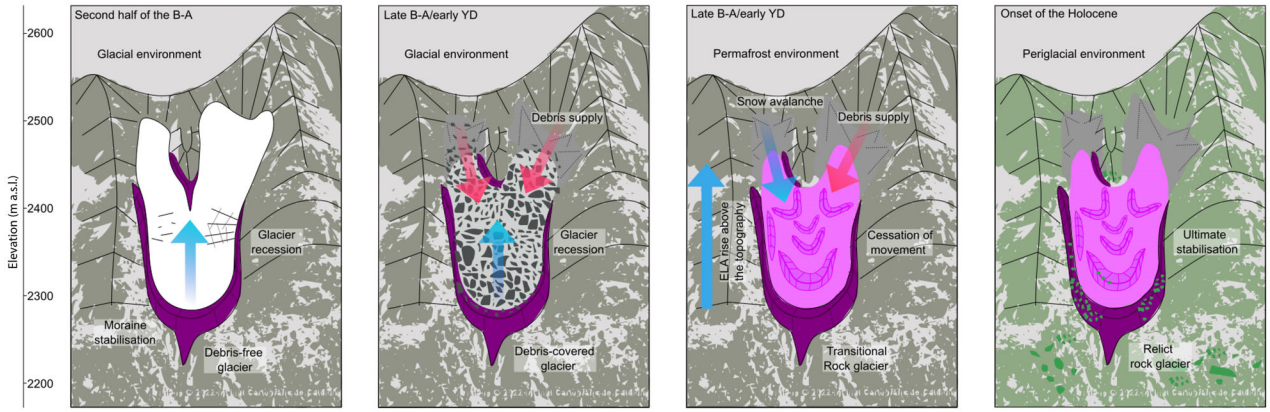

Fig. 5. Evolution model of the Lòcampo cirque. Development of the cirque moraine from a debris-free glacier during the second half of the Bølling–Allerød (B-A), succeeded by a debris-covered glacier. Following that, the debris-covered glacier evolved into a rock glacier that became stable during the late B-A/early Younger Dryas and finally relict by the onset of the Holocene, or afterwards.

Glacial and periglacial evolution of the Upper Garonne Basin during the T-1

During the Late Pleistocene glaciations, the Lòcampo cirque was fully glaciated and intensely shaped by glacial processes, as demonstrated by the palaeoglacier reconstruction of the entire Garonne catchment (Fernandes *et al.* 2017, 2021a). The Garonne palaeoglacier reached ~80 km long, with a maximum ice thickness of ~800 m, probably during, at least, the last two glacial cycles, as revealed by absolute dating applied to the glacial landforms and glaciolacustrine sediments in the terminal basin, at 420–440 m a.s.l. (Andrieu 1991; Fernandes *et al.* 2021a). During the LGM, the terminal basin was already deglaciated as suggested by two ^{10}Be ages from polished surfaces obtained at 18 km from the cirque moraine system (24.2±2.1 and 20.7±1.2 ka; Fernandes *et al.* 2021a). After the onset of the deglaciation, as in the rest of the Pyrenees, the Garonne palaeoglacier retreated to the highest valleys. In fact, the deglaciation of the Garonne catchment was underway until ca. 15–14 ka, when cirque floors under peaks of 2600–2700 m a.s.l. became entirely deglaciated, such as in Bacivèr cirque (Oliva *et al.* 2021). Similarly, in the surroundings of the Lòcampo cirque, the lowest polished bedrock surfaces in the Ruda Valley (1860 and 1900 m a.s.l.) showed similar ^{10}Be exposure ages of 15.0±0.9 and 13.8±0.8 ka (Fernandes *et al.* 2021b). The horizontal glacial retreat was parallel to ice thinning: polished surfaces between 140 and 30 m (2380–2260 m a.s.l.) above the Saboredo cirque floor reported ages of 14.8±0.9 and 14.0±0.8 ka. Therefore, considering the similar altitude of the cirque floor (2200–2300 m a.s.l.) and the prevailing aspect (W) of the Lòcampo cirque with respect to Bacivèr cirque, it is reasonable to assume that it was also probably ice free at 15–14 ka. In addition, this early deglaciation of Lòcampo cirque, and its small dimension (38 ha) within the context of the Garonne catchment cirques (62 ha on average), suggests a minimal glacial overdeepening, probably owing a lower ice thickness as result of its relatively low altitude and marginal position in the Ruda Valley.

Following the period of glacier recession until the first half of the B-A, glacial advances or standstills occurred during short-lived cold periods favouring glacier inception on the Lòcampo cirque floor, as shown by the samples from the cirque moraine that yielded a stabilization age of 13.2±1.1 ka. At the highest tributaries of the Upper Garonne Basin, glacial advances during the second half of the B-A have already been reported: in the Ruda Valley, glacial advances formed a moraine system with external (at 2080 m a.s.l.) and internal ridges (at 2190 m a.s.l.), dated at 13.5±0.9 and 13.0±0.8 ka, respectively (Fernandes *et al.* 2021b). To date, no other evidence of glacial activity during this period has been reported in the Upper Garonne Basin. Finally, it is important to stress that uncertainties of the moraine ages range from hundreds of years to a thousand years, which hampers accurate establishment of the timing of the glacial advance, especially when compared with periods shorter than that time scale.

Following the moraine stabilization within the Lòcampo cirque, a transition from debris-free to debris-covered glacier occurred probably during a very short period during the late B-A/early YD; however, we need more CRE ages to confirm the exact timing of this process. In fact, transitional landforms from debris-free to debris-covered glaciers have been shown to have formed in a few hundred years, as revealed by previous studies based on CRE (Fernández-Fernández *et al.* 2020; Palacios *et al.* 2020) and numerical simulations (Anderson *et al.* 2018). Similar results have been obtained in the Bacivèr cirque, where the evolution of a debris-free to debris-covered glacier could have occurred during the B-A/YD transition, becoming definitively stable during the Middle Holocene (Oliva *et al.* 2021).

The cirque moraine closes a relict rock glacier in the Lòcampo cirque with CRE ages ranging from 13.6±0.9 to 11.9±0.7 ka in three different ridges at 2280–2267, 2240–2235 and 2230–2220 m a.s.l. The thick debris mantle forming the Lòcampo rock glacier must have favoured a long preservation of the inner ice/permafrost, which may have delayed its complete stabilization that finally occurred during the onset of the Holocene, or afterwards. This wide range of CRE ages may also indicate a longer persistence of boulder adjustment, probably associated with buried ice that was favoured by the cold climate in North Iberia during the YD (Oliva *et al.* 2016; Rea *et al.* 2020). In fact, the cold and dry conditions may have favoured the persistence of permafrost within the rock glacier and boulder readjustment until its final stabilization at 11.9±0.7 ka. During this transitional state period the rock glacier front of the Lòcampo cirque corresponded to the lowest limit of the permafrost at ~2200 m a.s.l. Rock glaciers at similar elevations (1150–2250 m a.s.l.) represented 20% of all rock glaciers catalogued in Aran Valley (Fernandes *et al.* 2018). Considering an average lapse rate of 0.65 °C/100 m^{-1} and the −1/−2 °C on current active rock glaciers (Haeberli 1985), the mean annual air temperature at the front of the rock glacier of Lòcampo cirque would have been 3.6/4.6 °C less than today. This temperature is in agreement with the ELA-derived palaeotemperature reconstructions of 4.2 and 3.9 °C, estimated from the moraines dated by the B-A and B-A/YD transition in the Ruda Valley (Fernandes *et al.* 2021b).

Similar geomorphological evidence and geochronological data have also been reported in the neighbouring cirques, suggesting that during the late B-A/early YD glaciers were confined within the highest areas of the Upper Garonne Basin. However, depending on the local topography and the intensity of the paraglacial adjustment of the slopes, the deglaciation process followed different patterns:

- In wider cirques of the main valleys of the Garonne catchment with highest peaks of ~2700–2800 m a.s.l. glacial advances during the second half of the B-A have been reported: in the north-exposed Ruda Valley, glacial advances formed a moraine system with external (at 2080 m a.s.l.) and internal ridges (at 2190 m a.s.l.), dated at 13.5±0.9 and 13.0±0.8 ka, respectively (Fernandes *et al.* 2021b). However, determining the chronology of glacial advances during these centennial-scale events could be very challenging when using CRE and its associated uncertainties (Naughton *et al.* 2022). After such advances, glaciers completely vanished from the bottom of the cirques and left no periglacial features, as suggested by two polished surfaces above the moraine ridges (at 2310 and 2350 m a.s.l.) that yielded CRE ages of 12.7±0.8 and 12.8±0.8 ka (Fernandes *et al.* 2021b).
- In sheltered and lateral cirques with peaks at ~2600–2700 m a.s.l., small glaciers persisted or readvanced at the foot of the cirque walls forming moraines at ~2400 m a.s.l. during the onset of the YD. This is the case of the NE cirque of the Sendrosa Peak (2702 m a.s.l.), where a moraine yielded a mean CRE age of 12.6±1.3 ka (Fernandes *et al.* 2021b), or at the foot of the western rock wall of the Rosari Peak (2606 m a.s.l.), Bacivèr cirque, where a small cirque moraine was dated at 12.8±0.5 ka (Oliva *et al.* 2021). Within these moraines, cirque floors are covered with large chaotic deposits that suggest a gradual evolution towards periglacial environment with permafrost conditions: (i) longitudinal ridges and furrows suggest the existence of former debris-covered glaciers before its final deglaciation, such as in the Bacivèr cirque; and (ii) transversal ridges and furrows suggest the occurrence of rock glaciers, as occurs in the Sendrosa and Lòcampo cirques.

Chronology of the debris-free glacier to rock glacier transition in the Iberian Peninsula and its significance at the European scale

During the onset of the B-A, the climate in Europe was marked by rapid warming, with summer temperatures increasing by 2–3 °C and a 30% increase in precipitation. This trend was substituted by a gradual cooling of 2 °C until the end of the B-A interstadial (Lotter *et al.* 2012; von Grafenstein *et al.* 2013). The records of the $\delta^{18}O$ from lake sediment of Gerzensee, in the northern European Alps, demonstrated that centennial-scale episodes occurred by 14, 13.5 and 12.9 ka (von Grafenstein *et al.* 2013). These short-lived cold spells favoured the advance of glaciers in central Europe (Koinig *et al.* 2014). Such glacial advances built moraines that have been dated with different dating techniques, for the Scandinavian Ice Sheet (13.5–13.0 cal. ka BP; Mangerud *et al.* 2016), in the Black Forest (n = 2: 14.2±0.7 ka; Hofmann *et al.* 2022), in the eastern European Alps (n = 3: 14.4±1.0 ka; Braumann *et al.* 2022) and in the Tatra Mountains (n = 3: 13.4±0.5 ka; Engel *et al.* 2017), amongst other places.

In the case of the Iberian Peninsula, the $\delta^{18}O$ reconstructions from the Ostolo Cave revealed that the onset of the B-A was accompanied by a maximum temperature increase of 7.5 °C, which was subsequently followed by a gradual cooling (Bernal-Wormull *et al.* 2021). During this interstadial, the Iberian glaciers might have only persisted in the highest valleys of the Pyrenees (Oliva *et al.* 2022), where local topoclimatic conditions were more favourable to glacial maintenance (Fernandes *et al.* 2021b; Reixach *et al.* 2021). This is the case for the glacier in the Lòcampo cirque where the moraine was abandoned by the glacier (650 m long) and became stable by 13.2±1.1 ka. These glacial

standstills or advances can also correlate with short-lived cold reversals during the B-A interstadial recorded in Greenland ice cores (i.e. GI-1c and GI.1a; Rasmussen *et al*. 2014). However, owing to the intrinsic limitations of CRE dating on the uncertainty range, other dating techniques with higher precision are needed to support this linkage. The current available CRE ages in the Pyrenees show two periods of moraine formation during the second half of the B-A, where the oldest glacial advance has been reported in the central and eastern parts of the range at ~13.8–13.5 ka (Fernandes *et al*. 2021b; Reixach *et al*. 2021). This has been observed in moraines surrounding the glacial cirque in the Aránser Valley, Eastern Pyrenees, at 2200 m a.s.l. that reported a mean age of 13.6±0.9 ka (n = 3; Palacios *et al*. 2015b; Andrés *et al*. 2018; Reixach *et al*. 2021). Similar ages were recalculated from moraines in the Têt Valley at 2150 m a.s.l., 13.8±0.6 ka (n = 2; Delmas *et al*. 2008; Reixach *et al*. 2021). In the Central Pyrenees, a moraine from the Noguera Ribagorçana Valley (1560 m a.s.l.) yielded exposure ages of 13.7±0.9 ka (n = 3; Pallàs *et al*. 2006), and in the above-mentioned Ruda Valley (2080 m a.s.l.) at 13.5±0.9 ka (n = 2; Fernandes *et al*. 2021b). On the other hand, the youngest glacial advance during that phase was constrained at ~13.2–12.8 ka in the Têt Valley (n = 2: 13.1±0.6 ka; Reixach *et al*. 2021), Bacivèr cirque (n = 2: 12.8±0.5 ka; Oliva *et al*. 2021), Ruda Valley (n = 2: 13.0±0.8 ka; Fernandes *et al*. 2021b) and in the Soulcen Valley (n = 2: 13.2±0.3 ka; Jomelli *et al*. 2020). However, in the Lòcampo cirque, we have only found evidence of the second glacial phase (13.2–12.9 ka).

The glacier abandonment of the cirques in the Pyrenees favoured the formation of periglacial features in deglaciating areas, as probably occurred in the Lòcampo cirque. These shrinking glaciers became progressively covered with debris enhanced by periglacial or even paraperiglacial conditions (Mercier 2008). Past shifts in prevailing climate can determine the evolution of glaciers into debris-covered or rock glaciers (Anderson *et al*. 2018). Following glacial retreat during the second half of the B-A, enhanced debris supply would support the development of either debris-covered glaciers or rock glaciers during the late B-A/early YD. However, it is likely that the deglaciation in the Lòcampo cirque must have been different in each scenario. Longer deglaciation of the cirque would be expected for the formation of the debris-covered glacier compared with a rock glacier, as the ice content below the debris mantle is usually higher (85–45%; Janke *et al*. 2015). In fact, during the late B-A/early YD, sheltered cirques favoured glacier persistence next to the foot of rock walls from where boulders fed the debris-covered glacier (Fernandes *et al*. 2021a).

In the European mountains, the application of CRE dating on moraine boulders from debris-free and debris-covered glaciers revealed a scattered age distribution. This suggests an almost synchronous stabilization of the front with the recently abandoned (debris-free glacier) moraines, and in contrast, the upper sectors of the debris-covered glaciers became stable some millennia later. This delay might be related to the long period of boulder displacement triggered by the degradation of buried ice/permafrost that can persist for millennia trapped below the surface (Fernández-Fernández *et al*. 2017). In fact, the insulating effect of a debris mantle over buried ice can reduce ~40 times glacial ablation (Bosson & Lambiel 2016). This long-term stabilization has been detected in the deglaciated cirques during the T-1 (Fernández-Fernández *et al*. 2017; Oliva *et al*. 2021). In the Eastern Alps, a debris-covered glacier formed in the Norbert Valley at 1700 m a.s.l., within the limits of the area glaciated during the HS-1 (Gschnitz stadial), which became finally stable by ~16 ka (Steinemann *et al*. 2020). In the Sierra de la Demanda, Iberian Range, the transition from a debris-free to a debris-covered glacier was reconstructed in the Mencilla cirque through CRE ages from boulders belonging to moraines and a debris mantle located in less than 500 m from each other (1600–1700 m a.s.l.). The results showed synchronous stabilization during the Holocene Thermal Maximum, by 8–6 ka (Fernández-Fernández *et al*. 2017). As shown in the same study, a debris-covered glacier developed in the San Lorenzo cirque at 1800–1900 m a.s.l., between moraines attributed to the LGM and the HS-1; in this case, the authors proposed that activity definitively ceased by 8.7±0.8 ka (Fernández-Fernández *et al*. 2017). This pattern was also detected at the Bacivèr cirque, where a small debris-covered glacier at 2400–2500 m a.s.l. probably stopped moving by 7.2±0.5 ka (Oliva *et al*. 2021).

Despite the challenges in chronologically constraining the rapid transition into rock glaciers using CRE ages, our data set suggests that this process might have occurred during the late B-A/early YD. This study is the first at constraining rock glacier stabilization on the northern slope of the Pyrenees during the T-1, reinforcing the idea that rock glacier stabilization in the Iberian mountains was favoured by mild periods (interstadials), especially those at relatively low altitudes. In addition, the orientation might also be an important factor, as rock glaciers from the southern face of the Central Pyrenees dated with similar ages of ~13–11 ka are located at 100–200 m higher, at 2300–2400 m a.s.l. This is the example of the rock glaciers in the Piniecho (13.7±1.7 to 11.1±1.3 ka) and Catieras (12.5±1.3 to 11.6±1.4 ka) cirques (Palacios *et al*. 2015a, b).

The onset of the YD in Europe was a period of abrupt temperature decrease with a north–south gradient of 2–5 °C (Cacho *et al*. 2001; Moreno *et al*. 2014; Naughton *et al*. 2016) and a precipitation reduction of ~20% (Renssen *et al*. 2018). These climate conditions during this stadial favoured significant glacial advances in the northern and central European mountains (Palacios *et al*. 2023), as detected by different absolute dating techniques in the Scottish Highlands (e.g. Palmer

et al. 2020), Scandinavian mountains (e.g. Mangerud *et al.* 2016) or European Alps (e.g. Ivy-Ochs 2015). In the mountains surrounding the Mediterranean basin, the glacial advance was limited to the highest massifs, such as in Greece (e.g. Leontaritis *et al.* 2020) or in Turkey (e.g. Çiner *et al.* 2015).

On the Iberian Peninsula, the YD was marked by a decrease of ~5 °C as inferred from $\delta^{18}O$ values in the Ostolo Cave (Bernal-Wormull *et al.* 2021). These conditions were severe enough to maintain glaciers at the highest mountain ranges (Oliva *et al.* 2022) and also to promote periglacial activity under permafrost conditions in relatively low-altitude areas, such as in many Pyrenean cirques (Oliva *et al.* 2016). The chronological data derived from the application of CRE dating in rock glaciers are increasingly showing that most of the rock glaciers in the Iberian Peninsula had a paraglacial origin and became stable soon after their formation during the B-A interstadial (Palacios *et al.* 2012, 2015a, 2016, 2017b; Andrés *et al.* 2018; Jomelli *et al.* 2020; Santos-González *et al.* 2022). However, buried ice may have been preserved in transitional rock glaciers owing to the reduced ablation rate and nourishment of ice by snow avalanches (Bosson & Lambiel 2016; Anderson *et al.* 2018). Moreover, it is reasonable to assume that sheltered cirques had ideal topoclimatic conditions for the persistence of ice during the cold and dry YD stadial. Therefore, such cirques, where rock glaciers were previously developed, can probably indicate the areas where permafrost became finally preserved as is the case for the rock glacier in the Lòcampo cirque.

During the onset of the Holocene, the sea surface temperature in western Europe increased by about 2 °C in the Atlantic margin and >6 °C in the Mediterranean basin (Cacho *et al.* 2001). These warmer conditions led to a general rise of the periglacial belt in the highest mountain ranges of the Iberian Peninsula (Oliva *et al.* 2016). Higher temperatures must have favoured the gradual melting of the frozen masses, possibly buried glacial ice and permafrost layers, existing beneath the rock glacier of the Lòcampo cirque, which became relict. In fact, several rock glaciers in other Iberian ranges stabilized during the Holocene (Oliva *et al.* 2016). In the southern part of the Central Pyrenees, some rock glaciers ceased moving during the YD/Holocene transition. This occurred in the Piniecho and Catieras cirques (Gállego Valley), where stabilization of frontal lobes from different rock glaciers at ~2200–2400 m a.s.l. occurred at 12.6±1.6 to 11.1±1.3 ka and 12.5±1.3 to 11.6±1.4 ka, respectively (Palacios *et al.* 2015b). In the Eastern Pyrenees, CRE was also applied on the frontal lobe of an east-facing rock glacier at ~2400–2500 m a.s.l. in the La Pera cirque (Aránser Valley), which stabilized by 12.6±1.7 ka (Andrés *et al.* 2018). Finally, in Sierra Nevada, most rock glaciers stabilized at the end of the YD, such as in the Dílar Valley, where the north-facing rock glacier front (2600–3000 m a.s.l.) became stable by 11.4±1.0 ka (Palacios *et al.* 2016).

To conclude, the last deglaciation was a key period for rock glacier development in glacial cirques in mid-latitude European mountains. The geomorphological and chronological data showed that the glacial to periglacial transition was strongly controlled by climate, mainly during the interstadials. The deglaciation process triggered the formation of debris-covered glaciers and rock glaciers. Nevertheless, more robust data sets from periglacial features are needed to validate different scenarios, as the transition to periglacial conditions is highly influenced by the local topography that determines the environmental evolution in glacial cirques. This evolutionary sequence in the northern Central Pyrenees suggests a fast, even synchronous, transition from debris-free to debris-covered glacier, with accurate timing difficult to determine given the precision of the CRE dating. Following this glacial phase, mild conditions characterized the climate of transition from debris-covered glacier into a rock glacier that first stagnated by the B-A, and finally became relict by the onset of the Holocene. Finally, it is necessary to make larger efforts to better understand the limitations and strengths of the CRE dating on rock glaciers, which will provide valuable insights into the processes that forced rock glacier formation and stabilization during the glacial to periglacial transition.

Conclusions

Glacial and periglacial landforms are widespread features across the cirques of the Central Pyrenees, constituting the geomorphological record of environmental evolution during the last deglaciation. The present work brings a new eight-sample CRE data set from moraine and rock glacier boulders. The small Lòcampo cirque hosts a cirque moraine at ~2200–2300 m a.s.l. that was abandoned by a debris-free glacier during the second half of the B-A, at 13.2±1.1 ka. These ages agree well with other studies in the Pyrenees that report glacial advances/standstills during the second half of the B-A. Geomorphological evidence and CRE ages of 13.6±0.9 to 11.9±0.7 ka for the rock glacier do not allow its formation to be chronologically constrained and therefore we can only propose the following sequence: after the moraine stabilization, an intermediate phase of a debris-covered glacier formation occurred, which was followed by the rock glacier development and subsequent stabilization. Therefore, the stabilization of the rock glacier front occurred soon after its formation (13.6±0.9 ka) and became definitively relict during the onset of the Holocene (11.9±0.7 ka), or afterwards. The scattered rock glacier ages spanning up to *c.* 2–3 ka are indicative of the transition period towards its relict state, which was possibly delayed during the cold and dry YD, when boulders readjusted owing to the presence of buried ice (and permafrost) until its complete melting

(and thawing). This is a first attempt to constrain the evolutionary model of a debris-free glacier, debris-covered glacier and rock glacier in the Pyrenees and needs to be assessed with more precise chronological data to validate and extrapolate this model to other deglaciated mountain areas.

Acknowledgements. – This work was funded by the Research Group ANTALP (Antarctic, Arctic, Alpine Environments; 2017-SGR-1102), the Government of Catalonia and the Centro de Estudos Geográficos/IGOT – University of Lisbon (FCT I.P. UIDB/00295/2020 and UIDP/00295/2020). The research topics complement those of the project PALEOGREEN (CTM2017-87976-P) funded by the Spanish Ministry of Economy and Competitiveness and the project NUNANTAR funded by the Fundação para a Ciência e Tecnologia of Portugal (02/SAICT/2017-32002). Marcelo Fernandes holds a PhD fellowship of the Fundação para a Ciência e Tecnologia of Portugal (FCT – SFRH/139568/2018); Marc Oliva is supported by the Ramón y Cajal Program (RYC-2015-17597). ^{10}Be measurements were performed at the ASTER AMS national facility (CEREGE, Aix-en-Provence), which is supported by the INSU/CNRS and the ANR through the 'Projets thématiques d'excellence' programme for the 'Equipements d'excellence' ASTER-CEREGE action and Institut de recherche pour le développement (IRD). This research is also framed within the College on Polar and Extreme Environments (Polar2E) of the University of Lisbon. We also thank the National Park of Aigüestortes and Sant Maurici Lake for providing field access to the study sites and the reviewers for their constructive comments that helped to improve the quality of an earlier version of the manuscript. Finally, we thank the editor, Professor Jan A. Piotrowski, and the journal reviewers, professors Matteo Spagnolo and Philip Hughes, for their constructive comments during the revision process that allowed us to improve an earlier draft of the manuscript. The authors declare that they have no known competing financial interests or personal relationships that could have appeared to influence the work reported in this paper.

Author contributions. – MF: writing of the first draft of the manuscript, fieldwork leading, geomorphological analysis and mapping, laboratory tasks (sample processing, exposure age calculations) and data processing. MO: fieldwork, funding acquisition, geomorphological analysis, contribution to the writing, and revision of the final manuscript. JMF-F: fieldwork, geomorphological analysis, laboratory tasks (sample processing, exposure age calculations), contribution to the writing, and revision of the final manuscript. GV: funding acquisition, geomorphological analysis, contribution to the writing, and revision of the final manuscript. DP: fieldwork, theoretical conceptualization, geomorphological analysis, contribution to the writing, and revision of the final manuscript. JG-O: fieldwork, geomorphological analysis, contribution to the writing, and revision of the final manuscript. JV: fieldwork, geomorphological analysis, contribution to the writing, and revision of the final manuscript. IS: sample processing supervision, interpretation of the results and revision of the final manuscript. ASTER Team: AMS measurements of the ^{10}Be samples.

Data availability statement. – On behalf of the authors, I declare the data will be available to anyone interested any time on request.

References

Allard, J. L., Hughes, P. D. & Woodward, J. C. 2021: Heinrich Stadial aridity forced Mediterranean-wide glacier retreat in the last cold stage. *Nature Geoscience 14*, 197–205.

Amschwand, D., Ivy-Ochs, S., Frehner, M., Steinemann, O., Christl, M. & Vockenhuber, C. 2021: Deciphering the evolution of the Bleis Marscha rock glacier (Val d'Err, eastern Switzerland) with cosmogenic nuclide exposure dating, aerial image correlation, and finite element modeling. *The Cryosphere 15*, 2057–2081.

Anderson, R. S., Anderson, L. S., Armstrong, W. H., Rossi, M. W. & Crump, S. E. 2018: Glaciation of alpine valleys: the glacier – debris-covered glacier – rock glacier continuum. *Geomorphology 311*, 127–142.

André, M. F. 2002: Rates of postglacial rock weathering on glacially scoured outcrops (Abisko-Riksgränsen area, 68°N). *Geografiska Annaler: Series A, Physical Geography 84*, 139–150.

Andrés, N., Gómez-Ortiz, A., Fernández-Fernández, J. M., Tanarro, L. M., Salvador-Franch, F., Oliva, M. & Palacios, D. 2018: Timing of deglaciation and rock glacier origin in the southeastern Pyrenees: a review and new data. *Boreas 47*, 1050–1071.

Andrieu, V. 1991: *Dynamique du paléoenvironnement de la vallée montagnarde de la Garonne (Pyrénées Centrales, France) dela fin des temps glaciaires à l'actuel*. Ph.D. thesis, University of Toulouse, 330 pp.

Applegate, P. J., Urban, N. M., Keller, K., Lowell, T. V., Laabs, B. J. C., Kelly, M. A. & Alley, R. B. 2012: Improved moraine age interpretations through explicit matching of geomorphic process models to cosmogenic nuclide measurements from single landforms. *Quaternary Research 77*, 293–304.

Ballantyne, C. K. 2002: Paraglacial geomorphology. *In* Elias, S. A. (ed.): *Encyclopedia of Quaternary Science*, 553–565. Elsevier, Amsterdam.

Bernal-Wormull, J. L., Moreno, A., Pérez-Mejías, C., Bartolomé, M., Aranburu, A., Arriolabengoa, M., Iriarte, E., Cacho, I., Spötl, C., Edwards, R. L. & Cheng, H. 2021: Immediate temperature response in northern Iberia to last deglacial changes in the North Atlantic. *Geology 49*, 999–1003.

Bonsoms, J., Gonzalez, S., Prohom, M., Esteban, P., Salvador-Franch, F., López-Moreno, J. I. & Oliva, M. 2021: Spatio-temporal patterns of snow in the Catalan Pyrenees. *International Journal of Climatology 41*, 5676–5697.

Bosson, J. & Lambiel, C. 2016: Internal structure and current evolution of very small debris-covered glacier systems located in alpine permafrost environments. *Frontiers in Earth Science 4*, 39, https://doi.org/10.3389/feart.2016.00039.

Braucher, R., Guillou, V., Bourlès, D. L., Arnold, M., Aumaître, G., Keddadouche, K. & Nottoli, E. 2015: Preparation of ASTER in-house ^{10}Be/^{9}Be standard solutions. *Nuclear Instruments and Methods in Physics Research Section B: Beam Interactions with Materials and Atoms 361*, 335–340.

Braumann, S. M., Schaefer, J. M., Neuhuber, S. & Fiebig, M. 2022: Moraines in the Austrian Alps record repeated phases of glacier stabilization through the late Glacial and the early Holocene. *Scientific Reports 12*, 9438, https://doi.org/10.1038/s41598-022-12477-x.

Cacho, I., Grimalt, J. O., Canals, M., Sbaffi, L., Shackleton, N. J., Schönfeld, J. & Zahn, R. 2001: Variability of the western Mediterranean Sea surface temperature during the last 25,000 years and its connection with the Northern Hemisphere climatic changes. *Paleoceanography 16*, 40–52.

Capron, E., Rasmussen, S. O., Popp, T. J., Erhardt, T., Fischer, H., Landais, A., Pedro, J. B., Vettoretti, G., Grinsted, A., Gkinis, V., Vaughn, B., Svensson, A. M., Vinther, B. & White, J. W. C. 2021: The anatomy of past abrupt warmings recorded in Greenland ice. *Nature Communications 12*, 2106, https://doi.org/10.1038/s41467-021-22241-w.

Çiner, A., Sarikaya, M. A. & Yildirim, C. 2015: Late Pleistocene piedmont glaciations in the eastern Mediterranean; insights from cosmogenic ^{36}Cl dating of hummocky moraines in southern Turkey. *Quaternary Science Reviews 116*, 44–56.

Clark, D., Clark, M. M. & Gillespie, A. R. 1994: Debris-covered glaciers in the sierra Nevada, California, and their implications for snowline reconstructions. *Quaternary Research 41*, 139–153.

Clark, P. U., Dyke, A., Shakun, J. D., Carlson, A. E., Wohlfarth, B., Mitrovica, J., Hostetler, S. & McCabe, A. 2009: The Last Glacial Maximum. *Science 325*, 710–714.

Cochelin, B. 2017: *Champ de déformation du socle paléozoïque des Pyrénées*. Ph.D. thesis, University of Toulouse 3, 242 pp.

Crest, Y., Delmas, M., Braucher, R., Gunnell, Y. & Calvet, M. 2017: Cirques have growth spurts during deglacial and interglacial periods: evidence from ^{10}Be and ^{26}Al nuclide inventories in the central and eastern Pyrenees. *Geomorphology 278*, 60–77.

Delaloye, R. & Echelard, T. 2021: Towards standard guidelines for inventorying rock glaciers: baseline concepts (version 4.2). *In IPA Action Group Rock Glacier Inventories and Kinematics*. Available at: https://www3.unifr.ch/geo/geomorphology/en/research/ipa-action-group-rock-glacier.

Delmas, M., Gunnell, Y., Braucher, R., Calvet, M. & Bourlès, D. L. 2008: Exposure age chronology of the last glaciation in the eastern Pyrenees. *Quaternary Research 69*, 231–241.

Delmas, M., Gunnell, Y. & Calvet, M. 2015: A critical appraisal of allometric growth among alpine cirques based on multivariate statistics and spatial analysis. *Geomorphology 228*, 637–652.

Denton, G. H., Anderson, R. F., Toggweiler, J. R., Edwards, R. L., Schaefer, J. M. & Putnam, A. E. 2010: The last glacial termination. *Science 328*, 1652–1656.

Dlabáčková, T., Engel, Z., Uxa, T., Braucher, R. & ASTER Team 2023: ^{10}Be exposure ages and paleoenvironmental significance of rock glaciers in the Western Tatra Mts., Western Carpathians. *Quaternary Science Reviews 312*, 108147, https://doi.org/10.1016/j.quascirev.2023.108147.

Dunai, T. J. 2010: *Cosmogenic Nuclides: Principles, Concepts and Application in the Earth Surface Sciences*. Cambridge University Press, Cambridge, https://doi.org/10.1017/CBO9780511804519.

Dunne, J., Elmore, D. & Muzikar, P. 1999: Scaling factors for the rates of production of cosmogenic nuclides for geometric shielding and attenuation at depth on sloped surfaces. *Geomorphology 27*, 3–11.

Engel, Z., Mentlík, P., Braucher, R., Křížek, M., Pluháčková, M. & ASTER Team 2017: ^{10}Be exposure age chronology of the last glaciation of the Roháčská Valley in the Western Tatra Mountains, central Europe. *Geomorphology 293*, 130–142.

Fernandes, M., Oliva, M., Palma, P., Ruiz-Fernández, J. & Lopes, L. 2017: Glacial stages and post-glacial environmental evolution in the Upper Garonne valley, Central Pyrenees. *Science of the Total Environment 584–585*, 1282–1299.

Fernandes, M., Oliva, M., Vieira, G. & Lopes, L. 2022: Geomorphology of the Aran Valley (Upper Garonne Basin, Central Pyrenees). *Journal of Maps 18*, 219–231.

Fernandes, M., Oliva, M., Vieira, G., Palacios, D., Fernández-Fernández, J. M., Delmas, M., García-Oteyza, J., Schimmelpfennig, I., Ventura, J. & ASTER Team 2021a: Maximum glacier extent of the Penultimate Glacial Cycle in the Upper Garonne Basin (Pyrenees): new chronological evidence. *Environmental Earth Sciences 80*, 796, https://doi.org/10.1007/s12665-021-10022-z.

Fernandes, M., Oliva, M., Vieira, G., Palacios, D., Fernández-Fernández, J. M., Garcia-oteyza, J., Schimmelpfennig, I., ASTER Team & Antoniades, D. 2021b: Glacial oscillations during the Bølling–Allerød Interstadial–Younger Dryas transition in the Ruda Valley, Central Pyrenees. *Journal of Quaternary Science 37*, 42–58.

Fernandes, M., Palma, P., Lopes, L., Ruiz-Fernández, J., Pereira, P. & Oliva, M. 2018: Spatial distribution and morphometry of permafrost-related landforms in the Central Pyrenees and associated paleoclimatic implications. *Quaternary International 470*, 96–108.

Fernández-Fernández, J. M., Palacios, D., Andrés, N., Schimmelpfennig, I., Tanarro, L. M., Brynjólfsson, S., López-Acevedo, F. J., Sæmundsson, Þ. & ASTER Team 2020: Constraints on the timing of debris-covered and rock glaciers: an exploratory case study in the Hólar area, northern Iceland. *Geomorphology 361*, 107196, https://doi.org/10.1016/j.geomorph.2020.107196.

Fernández-Fernández, J. M., Palacios, D., García-Ruiz, J. M., Andrés, N., Schimmelpfennig, I., Gómez-Villar, A., Santos-González, J., Álvarez-Martínez, J., Arnáez, J., Úbeda, J., Léanni, L. & ASTER Team 2017: Chronological and geomorphological investigation of fossil debris-covered glaciers in relation to deglaciation processes: a case study in the Sierra de La Demanda, northern Spain. *Quaternary Science Reviews 170*, 232–249.

Frauenfelder, R., Laustela, M. & Kääb, A. 2005: Relative age dating of Alpine rockglacier surfaces. *Zeitschrift für Geomorphologie 49*, 145–166.

García-Ruiz, J. M., Palacios, D., Fernández-Fernández, J. M., Andrés, N., Arnáez, J., Gómez-Villar, A., Santos-González, J., Álvarez-Martínez, J., Lana-Renault, N. & Léanni, L. 2020: Glacial stages in the Peña Negra valley, Iberian Range, northern Iberian Peninsula: assessing the importance of the glacial record in small cirques in a marginal mountain area. *Geomorphology 362*, 107195, https://doi.org/10.1016/j.geomorph.2020.107195.

García-Ruiz, J. M., Palacios, D., González-Sampériz, P., De Andrés, N., Moreno, A., Valero-Garcés, B. L. & Gómez-Villar, A. 2016: Mountain glacier evolution in the Iberian Peninsula during the Younger Dryas. *Quaternary Science Reviews 138*, 16–30.

Gómez-Ortiz, A., Oliva, M., Salvador-Franch, F., Palacios, D., Tanarro, L. M., Sanjosé-Blasco, J. J. & Salvà-Catarineu, M. 2019: Monitoring permafrost and periglacial processes in Sierra Nevada (Spain) from 2001 to 2016. *Permafrost and Periglacial Processes 30*, 278–291.

González-García, M. 2014: *La alta montaña periglaciar en el Pirineo Central español: procesos, formas y condiciones ambientales*. Ph.D. thesis, University of Málaga. Available at: http://hdl.handle.net/10630/6973.

Gosse, J. C. & Phillips, F. M. 2001: Terrestrial in situ cosmogenic nuclides: theory and application. *Quaternary Science Reviews 20*, 1475–1560.

von Grafenstein, U., Belmecheri, S., Eicher, U., van Raden, U. J., Erlenkeuser, H., Andersen, N. & Ammann, B. 2013: The oxygen and carbon isotopic signatures of biogenic carbonates in Gerzensee, Switzerland, during the rapid warming around 14,685 years BP and the following interstadial. *Palaeogeography, Palaeoclimatology, Palaeoecology 391*, 25–32.

Haeberli, W. 1985: *Creep of Mountain Permafrost: Internal Structure and Flow of Alpine Rock Glaciers*. 142 pp. An der Eidgenossischen Technischen Hochschule Zurich, Herausgegeben von Prof. Dr. D. Vischer, Zurich.

Heiri, O., Koinig, K. A., Spötl, C., Barrett, S., Brauer, A., Drescher-Schneider, R., Gaar, D., Ivy-Ochs, S., Kerschner, H., Luetscher, M., Moran, A., Nicolussi, K., Preusser, F., Schmidt, R., Schoeneich, P., Schwörer, C., Sprafke, T., Terhorst, B. & Tinner, W. 2014: Palaeoclimate records 60-8 ka in the Austrian and Swiss Alps and their forelands. *Quaternary Science Reviews 106*, 186–205.

Hofmann, F. M., Preusser, F., Schimmelpfennig, I., Léanni, L. & ASTER Team 2022: Late Pleistocene glaciation history of the southern Black Forest, Germany: ^{10}Be cosmic-ray exposure dating and equilibrium line altitude reconstructions in Sankt Wilhelmer Tal. *Journal of Quaternary Science 37*, 688–706.

Hughes, P., Woodward, J. C. & Gibbard, P. 2006a: Quaternary glacial history of the Mediterranean mountains. *Progress in Physical Geography 3*, 334–364.

Hughes, P., Woodward, J. C. & Gibbard, P. 2006b: Late Pleistocene glaciers and climate in the Mediterranean. *Global and Planetary Change 50*, 83–98, https://doi.org/10.1016/j.gloplacha.2005.07.005.

Hughes, P. D. & Woodward, J. C. 2009: Glacial and Periglacial environments. *In* Woodward, J. (ed.): *The Physical Geography of the Mediterranean*, 353–383. Oxford University Press, Oxford, https://doi.org/10.1093/oso/9780199268030.003.0024.

Ivy-Ochs, S., 2015: Glacier variations in the European Alps at the end of the last glaciation. *Cuadernos de Investigacion Geografica 41*, 295–315.

Janke, J. R., Bellisario, A. C. & Ferrando, F. A. 2015: Classification of debris-covered glaciers and rock glaciers in the Andes of central Chile. *Geomorphology 241*, 98–121.

Jomelli, V., Chapron, E., Favier, V., Rinterknecht, V., Braucher, R., Tournier, N., Gascoin, S., Marti, R., Galop, D., Binet, S., Deschamps, C., Tissoux, H., Aumaître, G., Bourlès, D. L. & Keddadouche, K. 2020: Glacier fluctuations during the late glacial and Holocene on the Ariège valley, northern slope of the Pyrenees and reconstructed climatic conditions. *Mediterranean Geoscience Reviews 2*, 37–51.

Knight, J. 2019: A new model of rock glacier dynamics. *Geomorphology 340*, 153–159.

Knight, J., Harrison, S. & Jones, D. B. 2019: Rock glaciers and the geomorphological evolution of deglacierizing mountains. *Geomorphology 324*, 14–24.

Krautblatter, M., Funk, D. & Günzel, F. K. 2012: Why permafrost rocks become unstable: a rock-ice-mechanical model in time and space. *Earth Surface Processes and Landforms 38*, 876–887.

Lehmann, B., Anderson, R. S., Bodin, X., Cusicanqui, D., Valla, P. G. & Carcaillet, J. 2022: Alpine rock glacier activity over Holocene to

modern timescales (western French Alps). *Earth Surface Dynamics 10*, 605–633.
Leontaritis, A. D., Kouli, K. & Pavlopoulos, K. 2020: The glacial history of Greece: a comprehensive review. *Mediterranean Geoscience Reviews 2*, 65–90.
Li, Y. 2018: Determining topographic shielding from digital elevation models for cosmogenic nuclide analysis: a GIS model for discrete sample sites. *Journal of Mountain Science 15*, 939–947.
Lifton, N. A., Sato, T. & Dunai, T. J. 2014: Scaling in situ cosmogenic nuclide production rates using analytical approximations to atmospheric cosmic-ray fluxes. *Earth and Planetary Science Letters 386*, 149–160.
Lopes, L., Oliva, M., Fernandes, M., Pereira, P., Palma, P. & Ruiz-Fernández, J. 2018: Spatial distribution of morphometric parameters of glacial cirques in the Central Pyrenees (Aran and Boí valleys). *Journal of Mountain Science 15*, 2103–2119.
Lotter, A. F., Heiri, O., Brooks, S., van Leeuwen, J. F. N., Eicher, U. & Ammann, B. 2012: Rapid summer temperature changes during termination 1a: high-resolution multi-proxy climate reconstructions from Gerzensee (Switzerland). *Quaternary Science Reviews 36*, 103–113.
Mangerud, J., Aarseth, I., Hughes, A. L. C., Lohne, Ø. S., Skår, K., Sønstegaard, E. & Inge, J. 2016: A major re-growth of the Scandinavian Ice Sheet in western Norway during Allerød-Younger Dryas. *Quaternary Science Reviews 132*, 175–205.
Martin, L. C. P., Blard, P.-H., Balco, G., Lavé, J., Delunel, R., Lifton, N. A. & Laurent, V. 2017: The CREp program and the ICE-D production rate calibration database: a fully parameterizable and updated online tool to compute cosmic-ray exposure ages. *Quaternary Geochronology 38*, 25–49.
McColl, S. T. 2012: Paraglacial rock-slope stability. *Geomorphology 153–154*, 1–16.
Merchel, S. & Herpers, U. 1999: An update on radiochemical separation techniques for the determination of long-lived radionuclides via accelerator mass spectrometry. *Radiochimica Acta 84*, 215–219.
Merchel, S., Arnold, M., Aumaître, G., Benedetti, L., Bourlès, D. L., Braucher, R., Alfimov, V., Freeman, S. P. H. T., Steier, P. & Wallner, A. 2008: Towards more precise ^{10}Be and ^{36}Cl data from measurements at the 10-14 level: influence of sample preparation. *Nuclear Instruments and Methods in Physics Research, Section B: Beam Interactions with Materials and Atoms 266*, 4921–4926.
Mercier, D. 2008: Paraglacial and paraperiglacial landsystems: concepts, temporal scales and spatial distribution. *Géomorphologie: Relief, Processus, Environnement 14*, 223–233.
Moran, A. P., Ivy-Ochs, S., Vockenhuber, C. & Kerschner, H. 2016: Rock glacier development in the Northern Calcareous Alps at the Pleistocene-Holocene boundary. *Geomorphology 273*, 178–188.
Moreno, A., Svensson, A. M., Brooks, S. J., Connor, S., Engels, S., Fletcher, W. J., Genty, D., Heiri, O., Labuhn, I., Perşoiu, A., Peyron, O., Sadori, L., Valero-Garcés, B. L., Wulf, S. & Zanchetta, G. 2014: A compilation of Western European terrestrial records 60-8kaBP: towards an understanding of latitudinal climatic gradients. *Quaternary Science Reviews 106*, 167–185.
Naughton, F., Sanchez-Goñi, M. F., Landais, A., Rodrigues, T., Vázquez-Riveiros, N. & Toucanne, S. 2022: The Bølling-Allerød interstadial. *In* Palacios, D. (ed.): *European Glacial Landscapes*, 45–50. Elsevier, Amsterdam.
Naughton, F., Sanchez-Goñi, M. F., Rodrigues, T., Salgueiro, E., Costas, S., Desprat, S., Duprat, J., Michel, E., Rossignol, L., Zaragosi, S., Voelker, A. H. L. & Abrantes, F. 2016: Climate variability across the last deglaciation in NW Iberia and its margin. *Quaternary International 414*, 9–22.
Obase, T. & Abe-Ouchi, A. 2019: Abrupt Bølling-Allerød warming simulated under gradual forcing of the last deglaciation. *Geophysical Research Letters 46*, 11397–11405.
Oliva, M., Fernandes, M., Palacios, D., Fernández-Fernández, J. M., Schimmelpfennig, I., ASTER Team & Antoniades, D. 2021: Rapid deglaciation during the Bølling-Allerød interstadial in the Central Pyrenees and associated glacial and periglacial landforms. *Geomorphology 385*, 107735, https://doi.org/10.1016/j.geomorph.2021.107735.
Oliva, M., Mercier, D., Ruiz-Fernández, J. & McColl, S. 2019: Paraglacial processes in recently deglaciated environments. *Land Degradation & Development 31*, 1871–1876.
Oliva, M., Palacios, D. & Fernández-Fernández, J. M. (eds.) 2022: *Iberia, Land of Glaciers: How the Mountains were Shaped by Glaciers*. 618 pp. Elsevier, Amsterdam.
Oliva, M., Serrano, E., Gómez-Ortiz, A., González-Amuchastegui, M. J., Nieuwendam, A., Palacios, D., Pérez-Alberti, A., Pellitero, R., Ruiz-Fernández, J., Valcárcel, M., Vieira, G. & Antoniades, D. 2016: Spatial and temporal variability of periglaciation of the Iberian Peninsula. *Quaternary Science Reviews 137*, 176–199.
Palacios, D., Andrés, N., López-Moreno, J. I. & García-Ruiz, J. M. 2015a: Late Pleistocene deglaciation in the upper Gállego Valley, central Pyrenees. *Quaternary Research 83*, 397–414.
Palacios, D., de Andrés, N., Gómez-Ortiz, A. & García-Ruiz, J. M. 2017a: Evidence of glacial activity during the Oldest Dryas in the mountains of Spain. *Geological Society, London, Special Publications 433*, 87–110.
Palacios, D., de Andrés, N., de Marcos, J. & Vázquez-Selem, L. 2012: Glacial landforms and their paleoclimatic significance in Sierra de Guadarrama, Central Iberian Peninsula. *Geomorphology 139–140*, 67–78.
Palacios, D., García-Ruiz, J. M., Andrés, N., Schimmelpfennig, I., Campos, N., Léanni, L., Aumaître, G., Bourlès, D. L. & Keddadouche, K. 2017b: Deglaciation in the central Pyrenees during the Pleistocene–Holocene transition: timing and geomorphological significance. *Quaternary Science Reviews 162*, 111–127.
Palacios, D., Gómez-Ortiz, A., Andrés, N., Salvador-Franch, F. & Oliva, M. 2016: Timing and new geomorphologic evidence of the last deglaciation stages in Sierra Nevada (southern Spain). *Quaternary Science Reviews 150*, 110–129.
Palacios, D., Gómez-Ortiz, A., Andrés, N., Vázquez-Selem, L., Salvador-Franch, F. & Oliva, M. 2015b: Maximum extent of late Pleistocene glaciers and last deglaciation of La Cerdanya mountains, southeastern Pyrenees. *Geomorphology 231*, 116–129.
Palacios, D., Hughes, P. D., García-Ruiz, J. M. & Andrés, N. (eds.) 2022: *European Glacial Landscapes: Maximum Extent of Glaciations*. 546 pp. Elsevier, Amsterdam.
Palacios, D., Hughes, P. D., García-Ruiz, J. M. & Andrés, N. (eds.) 2023: *European Glacial Landscapes: The Last Deglaciation*. 644 pp. Elsevier, Amsterdam.
Palacios, D., Oliva, M., Gómez-Ortiz, A., Andrés, N., Fernández-Fernández, J. M., Schimmelpfennig, I., Léanni, L. & ASTER Team 2020: Climate sensitivity and geomorphological response of cirque glaciers from the late glacial to the Holocene, Sierra Nevada, Spain. *Quaternary Science Reviews 248*, 106617, https://doi.org/10.1016/j.quascirev.2020.106617.
Pallàs, R., Rodés, Á., Braucher, R., Carcaillet, J., Ortuño Candela, M., Bordonau, J., Bourlès, D. L., Vilaplana, J. M., Masana, E. & Santanach, P. 2006: Late Pleistocene and Holocene glaciation in the Pyrenees: a critical review and new evidence from ^{10}Be exposure ages, south-central Pyrenees. *Quaternary Science Reviews 25*, 2937–2963.
Palmer, A. P., Matthews, I. P., Lowe, J. J., Macleod, A. & Grant, R. 2020: A revised chronology for the growth and demise of Loch Lomond Readvance ('Younger Dryas') ice lobes in the Lochaber area, Scotland. *Quaternary Science Reviews 248*, 106548, https://doi.org/10.1016/j.quascirev.2020.106548.
Rasmussen, S. O., Bigler, M., Blockley, S. P., Blunier, T., Buchardt, S. L., Clausen, H. B., Cvijanovic, I., Dahl-Jensen, D., Johnsen, S., Fischer, H., Gkinis, V., Guillevic, M., Hoek, W. Z., Lowe, J., Pedro, J. B., Popp, T., Seierstad, I. K., Steffensen, J. P., Svensson, A. M., Vallelonga, P., Vinther, B. M., Walker, M., Wheatley, J. J. & Winstrup, M. 2014: A stratigraphic framework for abrupt climatic changes during the last glacial period based on three synchronized Greenland ice-core records: refining and extending the INTIMATE event stratigraphy. *Quaternary Science Reviews 106*, 14–28.
Rea, B. R., Pellitero, R., Spagnolo, M., Hughes, P. D., Ivy-Ochs, S., Renssen, H., Ribolini, A., Bakke, J., Lukas, S. & Braithwaite, R. J. 2020: Atmospheric circulation over Europe during the Younger Dryas. *Science Advances 6*, eaba4844, https://doi.org/10.1126/sciadv.aba4844.

Reixach, T., Delmas, M. & Calvet, M. 2021: Climatic conditions between 19 and 12 ka in the eastern Pyrenees, and wider implications for atmospheric circulation patterns in Europe. *Quaternary Science Reviews 260*, 106923, https://doi.org/10.1016/j.quascirev.2021.106923.

Renssen, H., Goosse, H., Roche, M. & Sepp, H. 2018: The global hydroclimate response during the Younger Dryas event. *Quaternary Science Reviews 193*, 84–97.

Rode, M. & Kellerer-Pirklbauer, A. 2012: Schmidt-hammer exposure-age dating (SHD) of rock glaciers in the Schöderkogel-Eisenhut area, Schladminger Tauern Range, Austria. *Holocene 22*, 761–771.

Santos-González, J., González-Gutiérrez, R. B., Redondo-Vega, J. M., Gómez-Villar, A., Jomelli, V., Fernández-Fernández, J. M., Andrés, N., García-Ruiz, J. M., Peña-Pérez, S. A., Melón-Nava, A., Oliva, M., Álvarez-Martínez, J., Charton, J. & Palacios, D. 2022: The origin and collapse of rock glaciers during the Bølling-Allerød interstadial: a new study case from the Cantabrian Mountains (Spain). *Geomorphology 401*, 108112, https://doi.org/10.1016/j.geomorph.2022.108112.

Scapozza, C., Lambiel, C., Bozzini, C., Mari, S. & Conedera, M. 2014: Assessing the rock glacier kinematics on three different timescales: a case study from the southern Swiss Alps. *Earth Surface Processes and Landforms 39*, 2056–2069.

Scherler, D. & Egholm, D. L. 2020: Production and transport of supraglacial debris: insights from cosmogenic ^{10}Be and numerical modeling, Chhota Shigri Glacier, Indian Himalaya. *Journal of Geophysical Research: Earth Surface 125*, 2020JF005586, https://doi.org/10.1029/2020JF005586.

Serrano, E., Agudo, C., Delaloye, R. & González-Trueba, J. J. 2001: Permafrost distribution in the Posets massif, Central Pyrenees. *Norsk Geografisk Tidsskrift 55*, 245–252.

Serrano, E., González-Trueba, J. J. & Sanjosé-Blasco, J. J. 2011: Dynamic, evolution and structure of Pyrenean rock glaciers. *Cuadernos de Investigacion Geografica 37*, 145–170.

Serrano, E., San José, J. J. & Agudo, C. 2006: Rock glacier dynamics in a marginal periglacial high mountain environment: flow, movement (1991–2000) and structure of the Argualas rock glacier, the Pyrenees. *Geomorphology 74*, 285–296.

Serrano, E., de Sanjosé-Blasco, J. J., Gómez-Lende, M., López-Moreno, J. I., Pisabarro, A. & Martínez-Fernández, A. 2019: Periglacial environments and frozen ground in the central Pyrenean high mountain area: ground thermal regime and distribution of landforms and processes. *Permafrost and Periglacial Processes 30*, 292–309.

Steinemann, O., Reitner, J. M., Ivy-Ochs, S., Christl, M. & Synal, H. A. 2020: Tracking rockglacier evolution in the Eastern Alps from the Lateglacial to the early Holocene. *Quaternary Science Reviews 241*, 106424, https://doi.org/10.1016/j.quascirev.2020.106424.

Styllas, M. N., Schimmelpfennig, I., Benedetti, L., Ghilardi, M., Aumaître, G., Bourlès, D. L. & Keddadouche, K. 2018: Late-glacial and Holocene history of the northeast Mediterranean mountains – new insights from in situ-produced ^{36}Cl-based cosmic ray exposure dating of paleo-glacier deposits on Mount Olympus, Greece. *Quaternary Science Reviews 193*, 244–265.

Tanarro, L. M., Palacios, D., Fernández-Fernández, J. M., Andrés, N., Oliva, M., Rodríguez-Mena, M., Schimmelpfennig, I., Brynjólfsson, S., Sæmundsson, Þ., Zamorano, J. J., Úbeda, J., Aumaître, G., Bourlès, D. L. & Keddadouche, K. 2021: Origins of the divergent evolution of mountain glaciers during deglaciation: Hofsdalur cirques, northern Iceland. *Quaternary Science Reviews 273*, 107248, https://doi.org/10.1016/j.quascirev.2021.107248.

Toucanne, S., Soulet, G., Freslon, N., Silva Jacinto, R., Dennielou, B., Zaragosi, S., Eynaud, F., Bourillet, J. F. & Bayon, G. 2015: Millennial-scale fluctuations of the European ice sheet at the end of the last glacial, and their potential impact on global climate. *Quaternary Science Reviews 123*, 113–133.

Uppala, S. M. and 45 others 2005: The ERA-40 re-analysis. *Quarterly Journal of the Royal Meteorological Society 131*, 2961–3012.

Vázquez-Riveiros, N., Toucanne, S., Rodrigues, T., Landais, A., Naughton, F. & Sanchez-Goñi, M. F. 2022: Definition of the last glacial cycle marine stages and chronology. *In* Palacios, D., Hughes, P., García-Ruiz, J. M. & Andrés, N. (eds.): *European Glacial Landscapes*, 171–173. Elsevier, Amsterdam.

Ventura, J. 2020: Spatial and temporal distribution of glaciers, debris-covered glaciers and rock glaciers during the last deglaciation in the Valley of the Bonaigua (Central Pyrenees). *Cuadernos de Investigación Geográfica 46*, 413–446.

Ward, G. K. & Wilson, S. R. 1978: Procedures for comparing and combining radiocarbon age determination: a critique. *Archaeometry 20*, 19–31.

Winkler, S. & Lambiel, C. 2018: Age constraints of rock glaciers in the Southern Alps/New Zealand – exploring their palaeoclimatic potential. *Holocene 28*, 778–790.